Article

Generation of functional oocytes from male mice in vitro

https://doi.org/10.1038/s41586-023-05834-x

Received: 3 November 2021

Accepted: 13 February 2023

Published online: 15 March 2023

Check for updates

Kenta Murakami[1,2], Nobuhiko Hamazaki[1], Norio Hamada[1,2], Go Nagamatsu[1], Ikuhiro Okamoto[3,4], Hiroshi Ohta[3,4], Yoshiaki Nosaka[3,4], Yukiko Ishikura[3,4], Tomoya S. Kitajima[5], Yuichiro Semba[6], Yuya Kunisaki[1,6], Fumio Arai[1], Koichi Akashi[6], Mitinori Saitou[3,4,7], Kiyoko Kato[2] & Katsuhiko Hayashi[1,8,9,10] ✉

Sex chromosome disorders severely compromise gametogenesis in both males and females. In oogenesis, the presence of an additional Y chromosome or the loss of an X chromosome disturbs the robust production of oocytes[1–5]. Here we efficiently converted the XY chromosome set to XX without an additional Y chromosome in mouse pluripotent stem (PS) cells. In addition, this chromosomal alteration successfully eradicated trisomy 16, a model of Down's syndrome, in PS cells. Artificially produced euploid XX PS cells differentiated into mature oocytes in culture with similar efficiency to native XX PS cells. Using this method, we differentiated induced pluripotent stem cells from the tail of a sexually mature male mouse into fully potent oocytes, which gave rise to offspring after fertilization. This study provides insights that could ameliorate infertility caused by sex chromosome or autosomal disorders, and opens the possibility of bipaternal reproduction.

Proper function and structure of sex chromosomes underlie sexual dimorphism in mammalian gametogenesis. In mice, primordial germ (PG) cells—the precursors of sperm and oocytes—arise at the extraembryonic region and migrate to the genital ridges, and then sex differentiation occurs in response to factors in the gonadal somatic environment[6]. Before reaching the gonads, PG cells are thought to be sexually bipotent, as they differentiate into either prospermatogonia or primary oocytes, depending on the gonadal somatic environment[7]. Despite this environment-dependent differentiation at the incipient stage, studies using mouse models of sex reversal have reported that XX PG cells were unable to eventually differentiate into spermatogonia[8], and XY PG cells differentiated into oocytes that had low fertility[1–5,9]. Further analyses revealed that the low potential of XY oocytes was attributable to mispairing of the heterogenous sex chromosomes[10,11] and/or ectopic expression of *Zfy2*, a Y-linked gene[1]. We confirmed the inability of sexually incompatible PG cells to undergo gametogenesis using an in vitro culture system for oocyte production from PS cells. In contrast to the robust production of functional oocytes from primordial germ cell-like (PGCL) cells derived from XX PS cells by aggregation with female gonadal somatic cells of embryonic day (E)12.5 embryos[12], oocyte production from XO and XY PS cells was severely impaired, even in the presence of female gonadal somatic cells, owing to the delay of meiotic initiation and asynapsis in both XO and XY oocytes, and the inhibitory effect of *Eif2s3y* in XY oocytes[13]. Together, this series of experiments reinforces that appropriate sex chromosomes in both germ cells and somatic cells are essential for proper gametogenesis. Thus, for oocyte production from cells with sex chromosome disorder, alteration of the chromosome set—that is, removal of the Y chromosome and/or duplication of the X chromosome—is essential.

Sex conversion in culture

As a model of the alteration of the chromosome set, we used BVSCN2 XY embryonic stem (ES) cells (129^{+Ter}/SvJ × C57BL/6 genetic background) harbouring *Blimp1*-mVenus (BV) (*Blimp1* is also known as *Prdm1*), a reporter gene of PG and PGCL cells, *stella*-ECFP (SC) (*stella* is also known as *Dppa3*), a reporter gene of PG and PGCL cells and oocytes. To monitor the number of X chromosomes in ES cells, a vector for DsRed expression was knocked into the X chromosome using the CRISPR–Cas9 system, generating BVSCN2 X^RY ES cells (Fig. 1a and Extended Data Fig. 1a). Because the two X chromosomes in mouse ES cells are both transcriptionally active, the number of X chromosomes could be determined by the difference in intensity of the fluorescent protein. We first tried to remove the Y chromosome by passaging a BVSCN2 X^RY ES cell clone. Consistent with previous findings that 1–3% of XY PS cells spontaneously lose their Y chromosome[14–16], we found that 6% (5 out of 87) of BVSCN2 X^RY ES cell subclones generated after 8 passages lost their Y chromosome (Extended Data Fig. 1b and Extended Data Table 1), thereby generating BVSCN2 X^RO ES cells. We next attempted to duplicate the X chromosome using BVSCN2 X^RO ES cells. Given that uniparental disomy of the X chromosome can be caused by unequal segregation of the X chromosomes into daughter cells[17–19], a similar machinery would be effective for generating XX ES cells from XO ES cells, but such segregation is quite rare. Fluorescence-activated cell

[1]Department of Stem Cell Biology and Medicine, Graduate School of Medical Sciences, Kyushu University, Fukuoka, Japan. [2]Department of Obstetrics and Gynecology, Graduate School of Medical Sciences, Kyushu University, Fukuoka, Japan. [3]Institute for the Advanced Study of Human Biology (ASHBi), Kyoto University, Kyoto, Japan. [4]Department of Anatomy and Cell Biology, Graduate School of Medicine, Kyoto University, Kyoto, Japan. [5]Laboratory for Chromosome Segregation, RIKEN Center for Biosystems Dynamics Research, Kobe, Japan. [6]Department of Medicine and Biosystemic Sciences, Graduate School of Medical Sciences, Kyushu University, Fukuoka, Japan. [7]Center for iPS Cell Research and Application (CiRA), Kyoto University, Kyoto, Japan. [8]Department of Genome Biology, Graduate School of Medicine, Osaka University, Suita, Japan. [9]Graduate School of Frontier Biosciences, Osaka University, Suita, Japan. [10]Premium Research Institute for Human Metaverse Medicine (WPI-PRIMe), Osaka University, Suita, Japan. ✉e-mail: hayashi.katsuhiko.104@m.kyushu-u.ac.jp

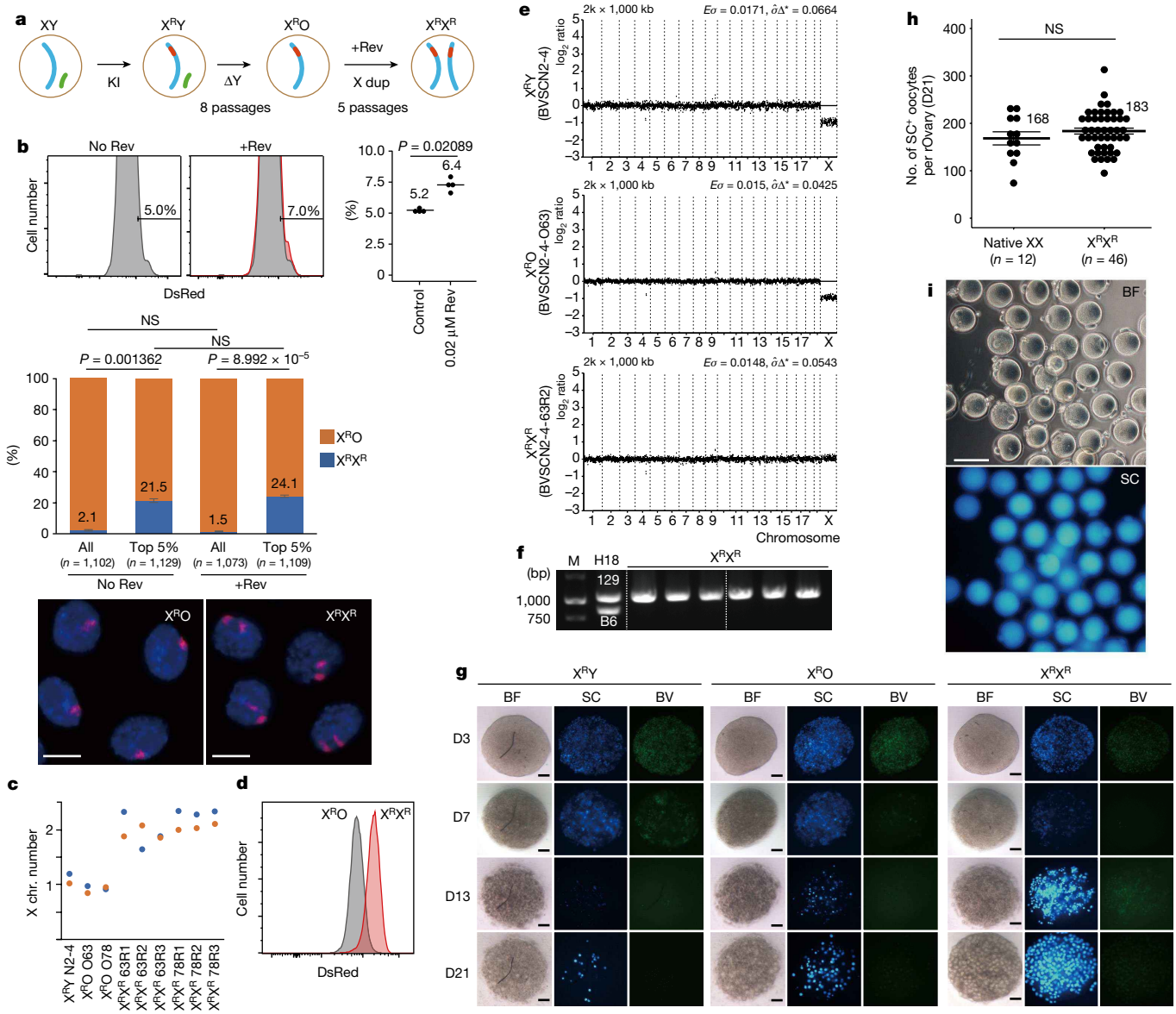

Fig. 1 | Sex conversion in ES cells and oocyte production in vitro. a, Schematic of procedure for sex conversion of ES cells. ΔY, Y chromosome deletion; KI, knock-in of marker gene into the X chromosome; Rev, reversine; X dup, X chromosome duplication. **b**, Isolation of XX ES cells from XO ES cells. Top, FACS analysis of BVSCN2 X^RO ES cells cultured without or with reversine, summarized in the graph on the right (biological quadruplicate experiments). Numbers in the graph denote the mean. Middle, the proportion of BVSCN2 X^RX^R ES cells in each fraction (all DsRed-labelled cells, or top 5% of DsRed-labelled cells) (biological triplicate experiments). Data are mean ± s.e.m. Bottom, DNA fluorescence in situ hybridization analysis of the X chromosome. Scale bars, 10 μm. Two-sided Welch's *t*-test. **c**, qPCR analysis of the X chromosome (chr.) number. Blue and orange dots show the X chromosome content (*Obp1a*) determined using chromosome 7 (*Omp*) and 11 (*Olfr1*, also known as *Or1e16*), respectively, as a reference. Clone IDs are shown along the *x* axis. **d**, FACS analysis of BVSCN2 X^RO and X^RX^R ES cells. **e**, DNA-seq analysis of sex-converted ES cells. Zero on the *y* axis is equivalent to two copies (log_2 ratio). The expected standard deviation ($E\sigma$) is defined as $\sqrt{(1/N)}$, where N is the average number of reads per bin. The measured standard deviation ($\sigma\Delta$) is calculated from the data with a mean-scaled and 0.1%-trimmed first-order estimate, prior to log_2-transforming the data for plotting. **f**, PCR analysis of SNPs in the X chromosome. The SfaNI recognition site is present only in B6 mice (Methods). H18 (XX ES cell line) has 129^{+Ter}/SvJ × C57BL/6 genetic background. Similar results were obtained in 14 ES cell lines. M, size marker. **g**, IVDi culture of rOvaries using BVSCN2 X^RY, X^RO and X^RX^R ES cells. Similar results were obtained in biological duplicate experiments. Days in culture are indicated with a D prefix. BF, bright field. Scale bars, 200 μm. **h**, The number of SC-positive oocytes per rOvary. Data are mean ± s.e.m. Two-sided Welch's *t*-test. Native XX: $n = 12$ rOvaries from 8 biologically independent experiments; X^RX^R: $n = 46$ rOvaries from 12 biologically independent experiments. **i**, MII oocytes from BVSCN2 X^RX^R ES cells. Scale bar, 100 μm. Similar results were obtained in experiments repeated more than ten times. NS, not significant.

sorting (FACS) followed by fluorescence in situ hybridization (FISH) analysis revealed that whereas 2.1 ± 0.4% (mean ± s.e.m.; $n = 3$, 1,102 cells in total) of X^RO ES cells became X^RX^R ES cells in all fractions, the ratio of X^RX^R ES cells increased significantly to 21.5 ± 1.2% (mean ± s.e.m.; $n = 3$, 1,129 cells in total) in the fraction with the top 5% of cells in terms of DsRed intensity (Fig. 1b). To further increase the efficiency, we used reversine, an inhibitor of the spindle assembly checkpoint that enhances missegregation[20]. Culturing ES cells with various concentrations of reversine revealed that an inhibitory effect on the proliferation of ES cells, possibly due to aneuploidy, was observed with 0.02 μM or higher concentrations of reversine (Extended Data Fig. 1c,d). We then examined whether reversine increased the DsRed-high population among

X^RO ES cells. As the cell cycle length of ES cells is 10 h or longer[21], we exposed X^RO ES cells to reversine for 10 h, so that no ES cells underwent mitosis more than twice. FACS analysis showed that as the concentration of reversine increased, the percentage of DsRed-high cells increased (Extended Data Fig. 1e). This trend was also observed for the G1 population, ruling out the possibility that the increased fluorescence was caused by the increase in the size of cells arrested at G2 (Extended Data Fig. 1e). ES cells treated with reversine concentrations of 0.1 μM or higher formed few and oddly shaped colonies; we therefore used 0.02 μM reversine in subsequent experiments. In X^RO ES cells treated with 0.02 μM reversine, the percentage corresponding to the top 5% fraction of DsRed-high X^RO ES cells without reversine treatment increased slightly but significantly to 6.35% on average. In the top 5% fractions of DsRed-high X^RO ES cells without or with reversine, the percentage of X^RX^R ES cells was similar, 21.5 ± 1.2% or 24.1 ± 0.6% (mean ± s.e.m., $n = 3$, 1,109 cells in total), respectively (Fig. 1b). These results indicate that a short-term (10 h) exposure to reversine has a positive, but not essential, effect in increasing the probability of separation of X^RX^R ES cells. In addition, in the top 0.02% of the DsRed-high population treated with reversine, all ES cells tested (6 out of 6) by comparative and quantitative PCR (qPCR) analysis were X^RX^R ES cells; these cells are hereafter termed BVSCN2 X^RX^R ES cells (Fig. 1c). FACS analysis showed that the DsRed intensity of the BVSCN2 X^RX^R ES cell clone was higher than that of X^RO ES cells (Fig. 1d). Finally, DNA-sequencing (DNA-seq) analysis confirmed that the 6 BVSCN2 X^RX^R ES cell clones were euploid, without any large insertions or deletions detectable at the resolution used in the analysis (Fig. 1e and Extended Data Fig. 1f). Duplication of the X chromosomes was confirmed by the result that both X chromosomes in all the BVSCN2 X^RX^R ES cell clones had single nucleotide polymorphisms (SNPs) specific for 129^{+Ter}/SvJ (Fig. 1f). These results demonstrated that euploid XX ES cells can be produced from ES cells harbouring any sex chromosome complement, such as XY and XO, by removal of the Y chromosome followed by duplication of the X chromosome.

Oocytes from the sex-converted XX ES cells

To test the ability of the sex-converted XX ES cells to undergo germ cell differentiation, we induced PGCL cells from BVSCN2 X^RX^R ES cells as well as parental BVSCN2 X^RY ES cells and BVSCN2 X^RO ES cells (Extended Data Fig. 2a). The induction rate was not different or higher in X^RX^R ES cells. Inactivation of the X chromosome was observed at a similar level to that in native XX ES cell derivatives[22], confirming the integrity of the reverted X chromosome during PGCL cell induction (Extended Data Fig. 2b). PGCL cells were then aggregated with E12.5 female gonadal somatic cells and cultured under an in vitro differentiation (IVDi) culture condition[12]. The number of SC-positive oocytes per reconstituted ovary (rOvary) from BVSCN2_X^RX^R ES cells at day 21 (183.7 ± 6.2, mean ± s.e.m.; $n = 46$) was clearly larger than those from parental BVSCN2 X^RY and BVSCN2 X^RO ES cells (Fig. 1g) and was not significantly different from that from native female ES cells (BVSCH18) (168.3 ± 13.8, mean ± s.e.m.; $n = 12$; $P = 0.328$, Welch's t-test) (Fig. 1h). Primary oocytes in the follicles isolated from rOvaries derived from BVSCN2 X^RX^R ES cells were differentiated into germinal vesicle (GV) oocytes after in vitro growth (IVG) and MII oocytes after in vitro maturation (IVM) (Fig. 1i). The MII ratio from GV oocytes using sex-converted XX ES cells was 30.9% (108 out of 349, Extended Data Table 2), a similar ratio to the one in a study using BVSCH18 cells[12] (28.9%, 923 out of 3,198; $P = 0.452$, Pearson's chi-square test). Gene expression analysis in GV oocytes and MII oocytes showed that the number of differentially expressed genes ($\log_2$ fold change >1, false discovery rate (FDR) <0.01) between BVSCN2 X^RX^R ES cell- and BVSCH18-derived oocytes was just 4 (Extended Data Fig. 2c), of which only *Parp8* is annotated as a protein-coding gene. It has not been reported that enforced expression of *Parp8*, as seen in the X^RX^R oocytes, has a critical effect on oogenesis in mice. Thus, we concluded that uniparental maternal disomy of the X chromosome from 129^{+Ter}/SvJ had no effect on oocyte development or gene expression.

Oogenesis from ES cells harbouring trisomy 16

Aneuploidy occurs frequently in ES cells[23,24], and we indeed observed trisomy 16 XY BVSC ES cells (XY+16 mosaic ES cells) (Extended Data Fig. 3a). Mice with segmental trisomy 16 have been used as a model of Down's syndrome[25], and thus BVSC XY+16 ES cells can be used as model of oogenesis in Down's syndrome. To test the effect of the additional chromosome 16 on oogenesis in vitro, we inserted a DsRed expression vector to the XY+16 mosaic ES cells, which were subcloned from single cells, and established an ES cell clone with trisomy 16 (BVSC X^RY+16 ES cells) (Fig. 2a,b). After 5 passages of the BVSC X^RY+16 ES cells, X^RO subclones lacking the Y chromosome (BVSC X^RO+16 ES cells) were picked up at a 3% frequency (3 out of 90) (Extended Data Table 1), and all three X^RO subclones still had trisomy 16 (Fig. 2b and Extended Data Fig. 3b). After reversine treatment, qPCR analysis showed that all clones ($n = 6$) picked up from the top 0.02% fraction of DsRed intensity had two X chromosomes (Extended Data Fig. 3c). DNA-seq of the 6 clones showed that 3 of them (50%) were XX+trisomy 16 (BVSC X^RX^R+16 ES cells), but the other 3 clones were completely euploid (BVSC X^RX^Reu ES cells) (Fig. 2b). This suggests that both the elimination of a chromosome 16 and duplication of the X chromosome occurred in the short period of culture in the ES cell line. To clarify the effect of reversine on the X chromosome and chromosome 16, we treated BVSC X^RO+16 ES cells with reversine at various concentrations, and the top 5% fraction of DsRed intensity and the total cell fraction were sorted separately and then analysed by DNA-seq. With reversine, the ratio of ES cells harbouring two X chromosomes was significantly increased in the top 5% fraction—compared with the total cell fraction—in a dosage-dependent manner, whereas the ratio of trisomy 16 did not significantly change (Extended Data Fig. 3d,e). We observed a similar trend in other euploid autosomes in the presence of 0.02 μM reversine, with no significant change in the missegregation rate in any autosomes. However, when 0.1 μM reversine was used, we observed a reproducible increase in the missegregation rate in certain autosomes, such as chromosomes 5, 9, 12 and 19 (Extended Data Fig. 3e). The apparent contradiction in 3 out of 6 subclones from the BVSC X^RX^R+16 ES cells being diploid whereas there was no significant change in the missegregation of chromosome 16 in the DNA-seq analysis may have been owing to the small number of subclones tested or the survival advantage of diploid cells under the culture conditions used for subcloning. Nevertheless, these results suggest that the X chromosome missegregation with 0.02 μM reversine is not accompanied by autosomal missegregation, reinforcing the suitability of this method for X chromosome duplication.

To investigate the effect of trisomy 16 on oogenesis, we performed oocyte induction. Trisomy 16 did not impair PGCL cell differentiation (Fig. 2c and Extended Data Fig. 3f), but most of the PGCL cells did not differentiate into primary oocytes. In sharp contrast, BVSC X^RX^Reu ES cells successfully differentiated into both PGCL cells and primary oocytes (Fig. 2d and Extended Data Fig. 3g). The number of SC-positive oocytes per rOvary at day 21 from BVSC X^RX^Reu ES cells was significantly higher than that from BVSC X^RX^R+16 ES cells (Fig. 2e). We differentiated primary oocytes from BVSC X^RX^Reu ES cells to MII oocytes (Fig. 2f and Extended Data Table 2). These results demonstrated that autosomal aneuploidy critically impaired oogenesis at an early stage during the IVDi period, but upon correction of the aneuploidy, the capacity for oogenesis in vitro was restored.

Oocytes from the sex-converted XX iPS cells

To strictly evaluate the function of oocytes from the sex-converted PS cells, the gold standard is whether or not they give rise to offspring. Moreover, it would expand the range of application if such functional

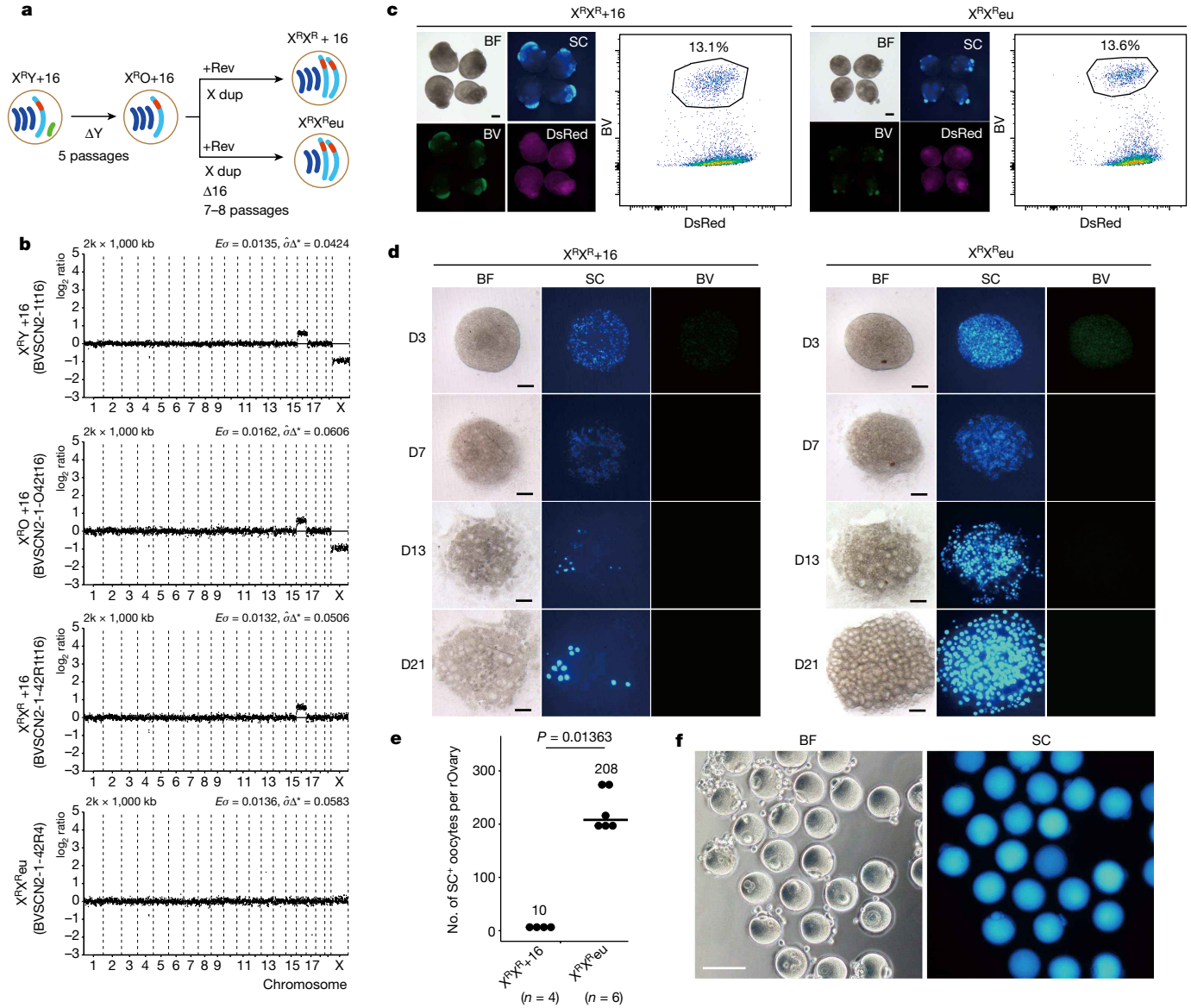

Fig. 2 | Oocyte production from XY ES cells with autosomal aneuploidy. **a**, Schematic of procedure for sex conversion and correction of autosomal aneuploidy in ES cells. Δ16, removal of a chromosome 16. **b**, DNA-seq analysis of trisomy 16 X^RY ES cells and derivatives. Zero on the *y* axis is equivalent to two copies (log_2 ratio). The genotype and the ID of individual clones are displayed along the *y* axis. **c**, PGCL cell induction from X^RX^R ES cells with or without trisomy 16. Representative images and FACS analyses of PGCL cells induced from sex-converted X^RX^R ES cells with or without trisomy 16 (X^RX^R+16 or X^RX^Reu, respectively). The percentage of PGCL cells is indicated. Note that trisomy 16 did not impair PGCL cell differentiation. Scale bars, 200 µm. **d**, IVDi culture using PGCL cells derived from X^RX^R+16 and X^RX^Reu ES cells. Representative images of rOvaries at the days indicated. Scale bars, 200 µm. **e**, The number of SC-positive oocytes per rOvary derived from X^RX^R+16 and X^RX^Reu ES cells at 21 days of culture. X^RX^R+16: $n = 4$ rOvaries from two independent cell lines; X^RX^Reu: $n = 6$ rOvaries from three independent cell lines. Numbers in the graph are the median. Two-sided Wilcoxon rank sum test. **f**, MII oocytes differentiated from X^RX^Reu. Scale bar, 100 µm. Similar results were obtained in biological triplicate experiments.

oocytes could be derived from male somatic cell-derived induced pluripotent stem (iPS) cells. Thus, we applied the sex conversion to iPS cells derived from tail tip fibroblasts of eight-week-old male mice (129X1/SvJ × C57BL/6J) harbouring BV but not SC (Fig. 3a). As described above, after insertion of DsRed into the X chromosome, thereby generating BV X^RY iPS cells (Extended Data Fig. 4a), followed by 9 subsequent passages, X^RO subclones (BV X^RO iPS cells) were detected at a 1.1% frequency (1 out of 91) (Extended Data Fig. 4b and Extended Data Table 1). After reversine treatment, qPCR showed that all clones ($n = 4$) picked up from top 0.02% fraction of DsRed intensity had two X chromosomes (Extended Data Fig. 4c). DNA-seq of four clones showed that the sex-converted XX iPS cells were euploid (Extended Data Fig. 4d); we termed these BV X^RX^R iPS cells. BV X^RX^R iPS cells were successfully differentiated to PGCL cells, primary oocytes, GV oocytes and MII oocytes in the same way as sex-converted XX ES cells (Fig. 3b–d, Extended Data Fig. 4e,f and Extended Data Table 2), whereas germ cell differentiation from parental BV X^RY iPS cells and BV X^RO iPS cells was severely disturbed during early oocyte development in the rOvay. BV X^RX^R iPS cell-derived MII oocytes were capable of fertilization with wild-type sperm in in vitro fertilization (IVF), and development to two-cell embryos (Fig. 3d and Extended Data Table 3). We transferred the two-cell embryos to pseudopregnant ICR mice and consequently 1.1% of embryos gave rise to pups (7 out of 630) (Fig. 3e and Extended Data Table 4). This developmental ratio of two-cell embryos was similar to that from tail tip fibroblast-derived XX iPS cells in a previous report[12] (0.6%, 8 out of 1,348; $P = 0.266$ by Fisher's exact test). All of the pups had dark eyes, resulting from the

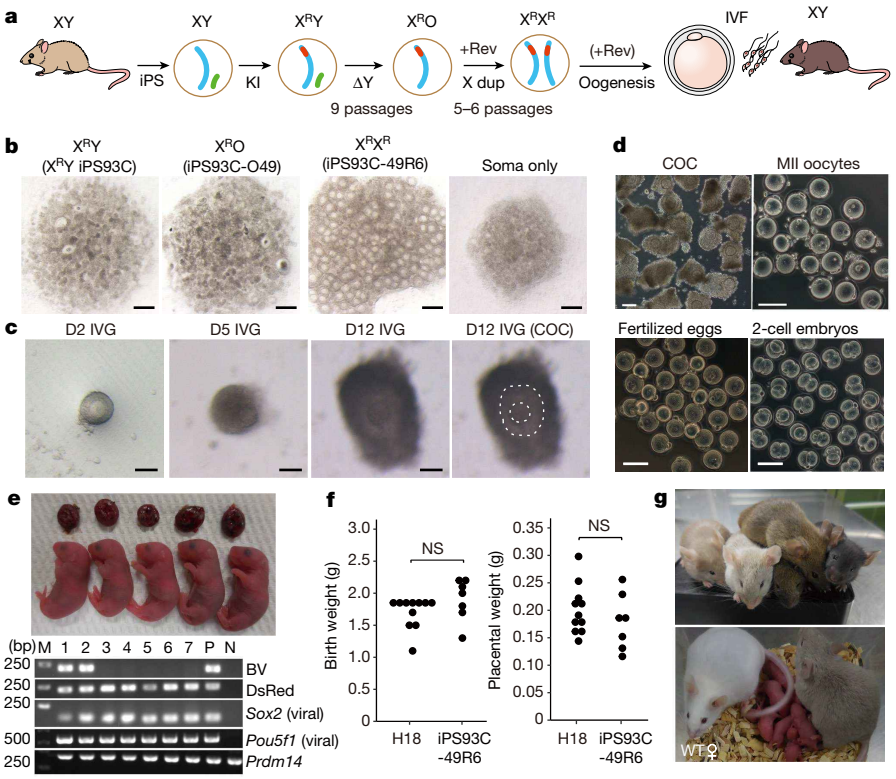

Fig. 3 | Pups from oocytes differentiated in vitro from sex-converted iPS cells. a, Schematic of the production of biparental offspring. **b**, rOvaries at day 21 of IVDi culture using X^RY, X^RO and X^RX^R iPS cells. Embryonic gonadal somatic cells were used as a negative control. The differentiation processes to obtain these rOvaries are shown in Extended Data Fig. 4f. Scale bars, 200 µm. Similar results were obtained in biological duplicate experiments. **c**, IVG culture using sex-converted iPS cells. Representative images from the days indicated. Far right, IVG-D12 image with the cumulus–oocyte complexes (COC) highlighted with dashed outlines. Scale bars, 100 µm. **d**, Maturation and fertilization of sex-converted oocytes. Scale bars, 100 µm. In **c**,**d**, similar results were obtained in experiments repeated more than ten times. **e**, Offspring from sex-converted iPS cells. Top, representative image showing pups and placentas obtained from sex-converted iPS cell-derived oocytes. Similar results were obtained in biological triplicate experiments. Bottom, genotyping of the seven pups obtained from three experiments (Extended Data Table 4). PCR products from BV and DsRed transgenes, exogenous retroviral *Sox2* and *Pou5f1* and the endogenous *Prdm14* (control) locus are shown. The positive (P) and negative (N) controls were the genomic DNA of iPS cells and ES cells, respectively. **f**, Birth weight (left) and placental weight (right) of offspring from the MII oocytes derived from sex-converted iPS cells and native XX ES cells (previous data[12]). H18: $n = 11$ independent mice and placentas; iPS93C-49R6: $n = 7$ independent mice and placentas. Two-sided Welch's *t*-test. **g**, Adult mice derived from iPS cells. Five of the seven mice (from **e**) at four weeks after birth (top) and a fertile adult male mouse (the grey one on the right; bottom) with offspring. Fertility was confirmed in all mice tested (one male and one female).

DsRed transgene and iPS markers (viral *Sox2* and *Pou5f1*), and some of the pups had the BV transgene (Fig. 3e). The birth weight and placental weight also resembled those in the previous report[12] (Fig. 3f). All of the pups grew up and fertility was conferred (Fig. 3g). On the basis of these results, we concluded that the oocytes from sex-converted iPS cells were functional.

Offspring from a single male iPS line

Given that XX iPS cells can be derived from XY iPS cells, it should be possible to generate offspring from a single male iPS line. This type of reproduction has previously been achieved by using XO ES cells[16], but it has never been accomplished through sex conversion in vitro. We therefore examined the generation of offspring derived from XY iPS cells and their sex-converted XX iPS cells by means of germline transmission in the chimeric mice. First, we injected BV X^RY iPS cells or BV X^RX^R iPS cells into BALB/c blastocysts to obtain chimeric mice. The ratio of grown male chimeric mice from BV X^RY iPS cells was 91% (20 out of 22 grown mice) and the ratio of grown female chimeric mice from BV X^RX^R iPS cells was 41% (14 out of 34 grown mice) (Extended Data Fig. 5a). Judging from the coat colour of offspring from a mating of the chimeric mice with wild-type BALB/c mice, the germline transmission rate of BV X^RY iPS cells was 100% (74 out of 74, $n = 6$ litters) and that of BV X^RX^R iPS cells was 97% (94 out of 97, $n = 10$ litters). iPS markers (*Sox2* and *Pou5f1*), X-linked-DsRed and BV were detectable in the non-albino offspring tested (Extended Data Fig. 5b). As the germline transmission was confirmed, intercrossed these chimeric mice (Extended Data Fig. 5c). To screen offspring derived from the iPS line, we examined H-2K haplotypes: C57BL/6J and 129X1/SvJ have H-$2K^b$, whereas BALB/c has H-$2K^d$. Four out of seventeen mice obtained from the intercrosses had only H-$2K^b$ (Extended Data Fig. 5d). This homozygosity was confirmed by SNPs at rs3022980 (T in C57BL/6J and 129X1/SvJ, and C in BALB/c) and at rs3022981 (T in C57BL/6J and 129X1/SvJ, and G in BALB/c). As expected, all four of the mice harbouring only the H-$2K^b$ haplotype had T at rs3022980 and rs3022981 (Extended Data Fig. 5e,f). All of the homozygous mice developed to adulthood (Extended Data Fig. 5g). These results demonstrated that offspring were generated from a single male iPS line via sex conversion in vitro.

XX ES cell isolation with a surface marker

This sex conversion system was highly reliant on the reporter integrated in the X chromosome, which limits application to other animals. We therefore attempted to identify an endogenous surface marker protein to distinguish XX ES and iPS cells from XO ES and iPS cells. Comparing the transcriptomes of XX ES cells and XO ES cells[13], we

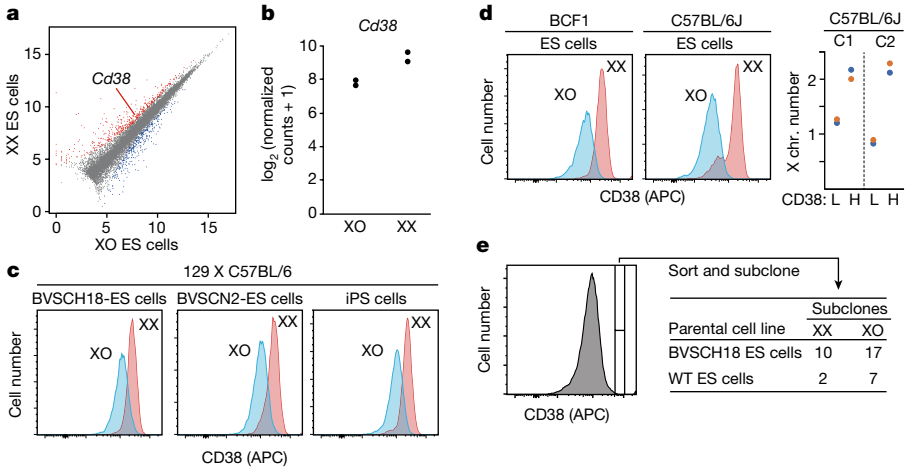

Fig. 4 | CD38 expression in XO and XX PS cells. a, Comparison of *Cd38* gene expression between XO ES cells and XX ES cells. The dot plot shows gene expression profiles of XO and XX ES cells, based on previous RNA-sequencing (RNA-seq) data[13]. Genes that are expressed more than 1.8-fold higher (red) or 1.8-fold lower (blue) in XX ES cells are shown. The FDR cutoff is 0.01. Biological duplicate samples. **b**, *Cd38* expression in XO and XX ES cells. The graph shows the expression level as $\log_2$(normalized counts + 1). Note that *Cd38* expression in XX ES cells was almost 2.9 times higher than that in XO ES cells. The expression profile is based on biological duplicate samples. **c**, FACS analysis of CD38 expression in XO and XX ES cells and iPS cells from 129X1/SvJ × C57BL/6 mice. **d**, FACS analysis of CD38 expression in XO and XX ES cells from BCF1 and C57BL/6J mice. Right, qPCR analysis of the X chromosome number in C57BL/6J (originally XX) ES cells. The CD38-low (L) population comprises XO ES cells. This suggests that C57BL/6J XX ES cells frequently lose a X chromosome. H, CD38-high (XX) cells. **e**, FACS and subcloning of CD38-high ES cells. Left, FACS plot showing the sorting gate.

could not identify an X-linked surface protein—for which an appropriate antibody was available—that was differentially expressed in an X-dosage-dependent manner. Instead, we found that the expression level of *Cd38*, a gene on chromosome 5 encoding a type II transmembrane glycoprotein, was 2.9 times higher in XX ES cells than in XO ES cells (Fig. 4a,b). FACS analysis showed that the fluorescence intensity of anti-CD38 antibody-conjugated with allophycocyanin (APC) of XX ES cells was higher than that of XO ES cells. This pattern was also observed in iPS cells and other strains (BCF1 and C57BL/6) (Fig. 4c,d). C57BL/6 ES cells exhibited two peaks, and qPCR analysis showed that some XX ES cells had lost the X chromosome (Fig. 4d and Extended Data Fig. 6a). The differential level of CD38 expression corresponded with that of DsRed between BVSCN2 X^RX^R ES cells and BVSCN2 X^RO ES cells (Extended Data Fig. 6b). On the basis of these results, we sorted from XO ES cells a population with high expression of CD38 at a level corresponding to that in XX ES cells (Extended Data Fig. 6c). As expected, qPCR revealed that 45% (10 out of 22) of the subclones derived from the population were XX clones. A cell population expressing CD38 at an even higher level than XX ES cells were not XX cells (0 out of 5) (Fig. 4e and Extended Data Fig. 6d). These outlier cells may have been generated by differentiation of ES cells. Nevertheless, we found CD38 to be a useful marker to distinguish XX ES cells from XO ES cells, and XX ES cell subclones could be successfully and efficiently isolated from XO ES cells by using the CD38 antibody followed by FACS. Using this method, we were able to isolate XX ES cells from a wild-type XO ES cell clone without the BVSC reporter with an efficiency of 22% (2 of 9 ES cell clones isolated) (Fig. 4e and Extended Data Fig. 6e). PGCL cells derived from the isolated XX ES cells could be identified by antibodies against SSEA1 and CD61 (Extended Data Fig. 6f), as reported previously[26]. Thus, a reporter construct is not required for sex conversion in mouse PS cells.

Discussion

Here we converted the sex of ES and iPS cells by removing the Y chromosome and duplicating the X chromosome. These sex-converted ES and iPS cells embody maternally uniparental disomy of the X chromosome with hybrid autosomes, making it possible to analyse the effect of uniparental disomy in oogenesis. The transcriptome of oocytes harbouring two maternal X chromosomes was not different from that of completely hybrid oocytes, in contrast to the clear transcriptomic difference between inbred and hybrid oocytes previously reported[27]. This in turn suggests that the contribution of X chromosome homozygosity to inbreeding depression is negligible, if it exists at all. However, we identified *Parp8* as a differentially expressed gene between sex-converted and native XX oocytes. Although there are no reports of increased *Parp8* expression having a negative effect on oogenesis, knockdown of all Parp family members (*Parp1* to *Parp16*) impairs the spindle and cortical poly(ADP-ribose) in mouse oocytes during meiosis[28]. Thus, attention should be given to the expression of Parp genes, especially in light of the possibility that genes in this family are susceptible to X chromosome homozygosity. Serial addition of autosomal homozygosity to ES and iPS cells will contribute to a better understanding of inbreeding depression in the developmental potential of oocytes. This seems feasible, since we were able to produce ES cells harbouring homozygosity on both the X chromosome and chromosome 16, and a previous study showed target chromosome elimination[29].

Autosomes in the sorted ES cells were largely unaffected following treatment with a low dose of reversine (0.02 μM) followed by cell sorting according to differential expression of a reporter gene or of CD38-enriched ES cells harbouring two maternal X chromosomes. This indicated that sex chromosome missegregation was not accompanied by autosomal missegregation. However, a higher dose of reversine (0.1 μM) resulted in a significant increase in missegregation in the X chromosome and some autosomes. Previous studies have also shown that some autosomal chromosomes—such as chromosomes 6, 8, 11, 12, 15 and 19—are prone to missegmentation in mouse ES cells, depending on the cell line and culture conditions[24,30,31]. These previous results, combined with the present study, indicate that individual autosomes have a distinct propensity for missegregation. It is known that chromosomal stability is highly dependent on the cell context. For example, one of the trisomic chromosomes is frequently lost during reprogramming to iPS cells from fibroblasts, but such loss is less frequent in fibroblasts per se[32]. Therefore, it would be of biological and clinical interest to examine the effect of reversine on X chromosome duplication in various somatic cell types that harbour XO, especially those that control sex differences, such as steroidogenic cells in the gonads. In this sense,

it should be noted that the resolution of the DNA-seq analyses in this study was not sufficient to detect point mutations and small structural variations in chromosomes, which frequently happen during passaging PS cells[33–35]. Therefore, a more rigorous evaluation of the effect of this method, which requires multiple passages, on genome integrity will be necessary for future research and application.

In this study, sex-converted XX iPS cells differentiated into functional oocytes, which gave rise to bipaternal offspring after fertilization and transplantation. Compared to relevant studies producing bipaternal offspring using haploid ES cells[36] or XO iPS cells[15], our strategy would be particularly advantageous from the following standpoints. First, the bipaternal offspring in our method did not show any apparent abnormalities or premature death, in sharp contrast to the offspring from haploid ES cells, which do not survive to adulthood. Second, the loss of one X chromosome causes a partial loss of fertility in mice[37] and substantial infertility in humans. Our method conferring two X chromosomes on PS cells will be able to overcome the infertility caused by XO and thus would be useful in a broader range of species, although there is a concern that doubling the X chromosome number would result in homozygous recessive X-linked mutations in the oocyte. From both a scientific and a technological viewpoint, alteration of the chromosome set in PS cells followed by oocyte production in culture provides a unique tool for studying the function of chromosomes on oogenesis, as well as for curing infertility due to sex chromosome or autosomal disorders. It would have been even more valuable if both eggs and sperm could have been produced in vitro from a single XY iPS cell and then fertilized to produce offspring. However, despite intensive experiments, which we repeated 12 times with more than 1,500 oocytes in total and sperm from the males that received iPS cell-derived spermatogonial stem cell-like cells as previously described[38], we were unable to obtain offspring owing to the low fertility potential of both oocytes and sperm produced in vitro. This is a technical limitation of this study, which could be overcome in future by refinement of culture conditions to improve the quality of in vitro-made gametes.

Online content

Any methods, additional references, Nature Portfolio reporting summaries, source data, extended data, supplementary information, acknowledgements, peer review information; details of author contributions and competing interests; and statements of data and code availability are available at https://doi.org/10.1038/s41586-023-05834-x.

1. Vernet, N. et al. The expression of Y-linked *Zfy2* in XY mouse oocytes leads to frequent meiosis 2 defects, a high incidence of subsequent early cleavage stage arrest and infertility. *Development* **141**, 855–866 (2014).
2. Amleh, A., Ledee, N., Saeed, J. & Taketo, T. Competence of oocytes from the B6.YDOM sex-reversed female mouse for maturation, fertilization, and embryonic development in vitro. *Dev. Biol.* **178**, 263–275 (1996).
3. Mahadevaiah, S. K., Lovell-Badge, R. & Burgoyne, P. S. Tdy-negative XY, XXY and XYY female mice: breeding data and synaptonemal complex analysis. *J. Reprod. Fertil.* **97**, 151–160 (1993).
4. Taketo-Hosotani, T., Nishioka, Y., Nagamine, C. M., Villalpando, I. & Merchant-Larios, H. Development and fertility of ovaries in the B6.YDOM sex-reversed female mouse. *Development* **107**, 95–105 (1989).
5. Lavery, R. et al. XY *Sox9* embryonic loss-of-function mouse mutants show complete sex reversal and produce partially fertile XY oocytes. *Dev. Biol.* **354**, 111–122 (2011).
6. Saitou, M. & Yamaji, M. Primordial germ cells in mice. *Cold Spring Harb. Perspect. Biol.* **4**, a008375 (2012).
7. Adams, I. R. & McLaren, A. Sexually dimorphic development of mouse primordial germ cells: switching from oogenesis to spermatogenesis. *Development* **129**, 1155–1164 (2002).
8. Koopman, P., Gubbay, J., Vivian, N., Goodfellow, P. & Lovell-Badge, R. Male development of chromosomally female mice transgenic for *Sry*. *Nature* **351**, 117–121 (1991).
9. Taketo, T. The role of sex chromosomes in mammalian germ cell differentiation: can the germ cells carrying X and Y chromosomes differentiate into fertile oocytes? *Asian J. Androl.* **17**, 360–366 (2015).
10. Taketo, T. & Naumova, A. K. Oocyte heterogeneity with respect to the meiotic silencing of unsynapsed X chromosomes in the XY female mouse. *Chromosoma* **122**, 337–349 (2013).
11. Alton, M., Lau, M. P., Villemure, M. & Taketo, T. The behavior of the X- and Y-chromosomes in the oocyte during meiotic prophase in the B6.Y(TIR)sex-reversed mouse ovary. *Reproduction* **135**, 241–252 (2008).
12. Hikabe, O. et al. Reconstitution in vitro of the entire cycle of the mouse female germ line. *Nature* **539**, 299–303 (2016).
13. Hamada, N. et al. Germ cell-intrinsic effects of sex chromosomes on early oocyte differentiation in mice. *PLoS Genet.* **16**, e1008676 (2020).
14. Yamamoto, S. et al. Rapid selection of XO embryonic stem cells using Y chromosome-linked GFP transgenic mice. *Transgenic Res.* **23**, 757–765 (2014).
15. Deng, J. M. et al. Generation of viable male and female mice from two fathers. *Biol. Reprod.* **84**, 613–618 (2011).
16. Eggan, K. et al. Male and female mice derived from the same embryonic stem cell clone by tetraploid embryo complementation. *Nat. Biotechnol.* **20**, 455–459 (2002).
17. Rudd, M. K. et al. Monosomy X rescue explains discordant NIPT results and leads to uniparental isodisomy. *Prenat. Diagn.* **38**, 920–923 (2018).
18. Luo, Y. et al. Uniparental disomy of the entire X chromosome in Turner syndrome patient-specific induced pluripotent stem cells. *Cell Discov.* **1**, 15022 (2015).
19. Denes, A. M., Landin-Wilhelmsen, K., Wettergren, Y., Bryman, I. & Hanson, C. The proportion of diploid 46,XX cells increases with time in women with Turner syndrome-a 10-year follow-up study. *Genet. Test. Mol. Biomarkers* **19**, 82–87 (2015).
20. Bolton, H. et al. Mouse model of chromosome mosaicism reveals lineage-specific depletion of aneuploid cells and normal developmental potential. *Nat. Commun.* **7**, 11165 (2016).
21. Nakai-Futatsugi, Y. & Niwa, H. Zscan4 is activated after telomere shortening in mouse embryonic stem cells. *Stem Cell Rep.* **6**, 483–495 (2016).
22. Hayashi, K. et al. Offspring from oocytes derived from in vitro primordial germ cell-like cells in mice. *Science* **338**, 971–975 (2012).
23. Codner, G. F. et al. Aneuploidy screening of embryonic stem cell clones by metaphase karyotyping and droplet digital polymerase chain reaction. *BMC Cell Biol.* **17**, 30 (2016).
24. Gaztelumendi, N. & Nogues, C. Chromosome instability in mouse embryonic stem cells. *Sci Rep.* **4**, 5324 (2014).
25. Roper, R. J., St John, H. K., Philip, J., Lawler, A. & Reeves, R. H. Perinatal loss of Ts65Dn Down syndrome mice. *Genetics* **172**, 437–443 (2006).
26. Hayashi, K., Ohta, H., Kurimoto, K., Aramaki, S. & Saitou, M. Reconstitution of the mouse germ cell specification pathway in culture by pluripotent stem cells. *Cell* **146**, 519–532 (2011).
27. Severance, A. L., Midic, U. & Latham, K. E. Genotypic divergence in mouse oocyte transcriptomes: possible pathways to hybrid vigor impacting fertility and embryogenesis. *Physiol. Genomics* **52**, 96–109 (2020).
28. Xie, B. et al. Poly(ADP-ribose) mediates asymmetric division of mouse oocyte. *Cell Res.* **28**, 462–475 (2018).
29. Zuo, E. et al. CRISPR/Cas9-mediated targeted chromosome elimination. *Genome Biol.* **18**, 224 (2017).
30. Choi, J. et al. Prolonged Mek1/2 suppression impairs the developmental potential of embryonic stem cells. *Nature* **548**, 219–223 (2017).
31. Zhang, M. et al. Aneuploid embryonic stem cells exhibit impaired differentiation and increased neoplastic potential. *EMBO J.* **35**, 2285–2300 (2016).
32. Hirota, T. et al. Fertile offspring from sterile sex chromosome trisomic mice. *Science* **357**, 932–935 (2017).
33. Liu, P. et al. Passage number is a major contributor to genomic structural variations in mouse iPSCs. *Stem Cells* **32**, 2657–2667 (2014).
34. Young, M. A. et al. Background mutations in parental cells account for most of the genetic heterogeneity of induced pluripotent stem cells. *Cell Stem Cell* **10**, 570–582 (2012).
35. Liang, Q., Conte, N., Skarnes, W. C. & Bradley, A. Extensive genomic copy number variation in embryonic stem cells. *Proc. Natl Acad. Sci. USA* **105**, 17453–17456 (2008).
36. Li, Z. K. et al. Generation of bimaternal and bipaternal mice from hypomethylated haploid ESCs with imprinting region deletions. *Cell Stem Cell* **23**, 665–676.e664 (2018).
37. Vaz, B., El Mansouri, F., Liu, X. & Taketo, T. Premature ovarian insufficiency in the XO female mouse on the C57BL/6J genetic background. *Mol. Hum. Reprod.* **26**, 678–688 (2020).
38. Ishikura, Y. et al. In vitro derivation and propagation of spermatogonial stem cell activity from mouse pluripotent stem cells. *Cell Rep.* **17**, 2789–2804 (2016).

Methods

Data reporting
No statistical methods were used to predetermine sample size. The experiments were not randomized, as we tested all available samples. The investigators were not blinded to allocation during experiments and outcome assessment.

Animals
All animal experiments were approved by the Institutional Animal Care and Use Committee at Kyushu University (no. A20-026-1 and no. 20-009-1). All animal experiments followed all relevant guidelines and regulations of Kyushu University for animal use. ICR, C57BL/6, 129X1/SvJ and BALB/c mice were purchased from Japan SLC. E12.5 gonadal somatic cells were collected from ICR embryos. All mice were maintained in constant temperature (22–25 °C) and humidity (50–70%) under a 12 h light:12 h dark cycle with light onset at 08:00.

ES cells and iPS cells
BVSC ES cells were established as described previously[12,13]. BVSCN2 cells are XY ES cells, BVSCH18 cells are XX ES cells and BVSCH18 39RC4 cells are XO ES cells. BV iPS cells were generated from tail tip fibroblasts of male BV hybrid mice (129X1/SvJ × C57BL/6J) by introducing retroviral vectors containing *Pou5f1*, *Sox2*, *Klf4* and *Myc*[12]. BCF1 ES cells were reported previously[39]. Both C57BL/6J and reporter-free 129X1/SvJ × C57BL/6J ES cells were established in our laboratory from the blastocysts. These ES and iPS cells were maintained under a 2i/LIF condition without feeder cells[40]. The ES and iPS cell lines in this study were not tested for mycoplasma contamination.

Transfection
DsRed was knocked into the X chromosome of ES and iPS cells using a CRISPR–Cas9 system as described previously[13]. The targeting vector pTk-SCEC-HS1-XSL1 with the pX330 expressing the guide RNA (gRNA) was transfected into ES and iPS cells. Genomic DNA was isolated from the transfected ES and iPS cells by phenol/chloroform extraction. The DNA extracted was amplified by PCR and then subjected to gel electrophoresis. The expected sizes of PCR fragments were 11,148 bp for the transfected cells and 6,901 bp for wild-type cells. The primers and gRNA used in this study are shown in Supplementary Table 1.

DNA FISH analysis
ES cells cultured on a glass coverslip coated with 0.01% poly-L-ornithine (Sigma) and 300 ng ml^{-1} laminin (BD Biosciences)[41] were washed twice in PBS (Wako). The coverslips were fixed in 3:1 methanol/glacial acetic acid two times for 10 min each time. After the coverslips were dried, they were denatured with X chromosome probes (MetaSystems D-1420-050-OR) for 5 min at 75 °C and then hybridized for 16 h at 37 °C. The coverslips were washed in 50% formamide-containing 2× SSC 3 times for 7 min at 42 °C, washed in 2× SSC twice for 5 min at 42 °C, stained with DAPI (1 μg ml^{-1} in 2× SSC) for 3 min at room temperature, and then washed in 2× SSC for 5 min at room temperature. The coverslips and slides were mounted in Fluoro-KEEPER Antifade Reagent (Nacalai Tesque) for analysis using a BZ-X700 fluorescence microscope (KEYENCE).

Effect of reversine on the proliferation of ES cells
ES cells were cultured with reversine (BioVision) on one well of a 12-well plate with mitomycin-treated mouse embryonic fibroblasts (MEFs) and passaged every other day. The cell number was counted at every passage and 1×10^5 ES cells or all ES cells (in cases with less than 1×10^5) were passaged. To examine the short-term effect of reversine, ES cells were cultured with reversine for 10–12 h and then without reversine for 36 h. At day 2, the cell number was counted and the cells were analysed by FACS.

Fluorescence intensity and cell cycle analysis
DsRed ES cells after reversine treatment were run on a FACSAria SORP cell sorter with FACSDiva v6.1.3 software (BD Biosciences). For the cell cycle analysis, ES cells were incubated with Vybrant DyeCycle Violet stain (Invitrogen) at 37 °C for 30 min before FACS analysis. The population around the high peak in violet was set as the G1 phase and the DsRed intensity of the population was analysed.

Generation of XO ES and iPS cells from XY ES and iPS cells
Genotyping for sex chromosomes was performed as described previously[12]. PCR amplified a 253-bp fragment from the X chromosome and 355-bp and 399-bp fragments from the Y chromosome. Sex chromosomes were confirmed by PCR and gel electrophoresis, and XY ES and iPS cells were passaged several times and then subcloned. Each subclone that showed only the shorter band (253-bp fragment) by gel electrophoresis was used as XO ES or iPS cells. The primers used for genotyping are shown in Supplementary Table 1.

Generation of XX ES and iPS cells from XO ES and iPS cells treated with reversine
DsRed XO ES and iPS cells after 0.02 μM reversine treatment were sorted by the gate set at the top 0.02% of control ES and iPS cells using a BD FACSAria SORP or Fusion cell sorter with FACSDiva v8 or v9 software (BD Biosciences). The sorted ES and iPS cells were subcloned on the culture plate. Round, dome-shaped colonies were selected. Each clone was examined by qPCR and DNA-seq analysis.

Determination of the X chromosome copy number
The X chromosome copy number was determined by qPCR as described[42]. In brief, a primer pair for the *obp1a* gene was used to quantify the X chromosome content, with two primer pairs for the *Omp* gene (Chr 7) and *Olfr1* gene (Chr 11) used as an autosomal reference. Genomic DNA of XO ES cells (BVSCH18 39RC4)[13] was used as a reference. Genes of interest were amplified with Power SYBR Green PCR Master Mix (Applied Biosystems) using a CFX384 Touch Real-Time PCR Detection System (Bio-Rad Laboratories). The primers used for qPCR are shown in Supplementary Table 1.

Determination of the autosomal copy number
The autosomal copy number was determined as described[43]. In brief, libraries were prepared using Nextera DNA Flex Library Prep (Illumina) according to the manufacturer's instructions, and sequenced on a NextSeq 500 DNA sequencer (75 bp single; Illumina). After trimming of the adapter sequences and low-quality bases with Trimmomatic v.0.38[44], the processed reads were mapped to mouse genome mm10 (https://jp.support.illumina.com/sequencing/sequencing_software/igenome.html) using Burrows–Wheeler Aligner (BWA) v.0.7.17[45]. Generated BAM files were sorted and indexed using samtools v.1.9[46]. PCR duplicates were removed with Picard v.2.18.12. Generated BAM files were analysed using QDNAseq v.1.26.0[43] in R v 4.0.4.

Analysis of the X chromosome origin
The X chromosome origin was determined as described previously[13]. PCR and SfaNI digestion generated a 1,064-bp fragment in 129/SvJ and 845-bp and 219-bp fragments in C57BL/6. The primers used in this study are shown in Supplementary Table 1.

PGCL cell induction and formation of reconstituted ovaries
PGCL cell induction was performed as described previously[41]. E12.5 female gonadal somatic cells were collected by strictly removing endogenous PG cells with MACS using both SSEA1 and CD31 antibodies according to the manufacturer's instructions (Miltenyi Biotec). PGCL cells were purified by a FACSAria SORP or Fusion cell sorter and aggregated with E12.5 female gonadal somatic cells in a low-binding U-bottom 96-well

plate (NUNC or Greiner) for 2 days of culture in GK15 medium containing 1 μM retinoic acid (Sigma) and 10 μM Y27632 (Wako). A total of 5,000 PGCL cells and 75,000 gonadal somatic cells were cultured to form one reconstituted ovary (rOvary). The antibodies for MACS separation in this study are shown in Supplementary Table 2.

IVDi culture

IVDi culture was performed as described[47]. rOvaries were placed on Transwell-COL membranes (Costar) or collagen type I and type III (Nippi)-precoated VECELL membranes (Vessel) soaked in αMEM-based IVDi medium (αMEM (Gibco) supplemented with 2% FCS (Gibco), 150 μM ascorbic acid (Sigma), 1× GlutaMAX (Gibco), 1× penicillin/streptomycin (Gibco) and 55 μM 2-mercapthoethanol (Gibco)). At day 4 of culture, the culture medium was changed to StemPro-34-based IVDi medium (StemPro-34 SFM (Gibco) supplemented with 10% FCS, 150 μM ascorbic acid, 1× GlutaMAX, 1× penicillin/streptomycin and 55 μM 2-mercapthoethanol). From days 7 to 10, 500 nM ICI182,780 (Tocris) was added to the StemPro-34-based IVDi medium. In the following culture, the medium was changed every other day. At day 21, the number of SC-positive oocytes was counted.

IVG culture

At day 21 of IVDi culture, individual secondary follicles were manually dissociated using a sharpened tungsten needle in IVG manipulation medium (αMEM (Gibco or Nacalai Tesque) supplemented with 5% FCS, 1× penicillin/streptomycin, and 20 mM HEPES (Gibco)). The isolated secondary follicles on the Transwell-COL membranes were soaked in IVG medium (αMEM supplemented with 5% FCS, 2% polyvinylpyrrolidone (Sigma), 150 μM ascorbic acid, 1× GlutaMAX, 1× penicillin/streptomycin, 100 μM 2-mercapthoethanol, 55 μg ml^{-1} sodium pyruvate (Nacalai Tesque), and 0.1 IU ml^{-1} FSH (Merck)) with 15 ng ml^{-1} BMP15 (R&D Systems) and 15 ng ml^{-1} GDF9 (R&D Systems). At day 2 of culture, BMP15 and GDF9 were withdrawn from the medium. At day 3 of culture, IVG medium was added to cover the follicles. At day 4 of culture, the follicles were incubated in 0.1% collagenase type I (Worthington Biochemical Corporation) for 10 min at 37 °C, washed three times with αMEM supplemented with 5% FCS, and cultured in IVG medium. In the following culture, the medium was changed every other day. At day 12 of culture, COCs grown on the membrane were collected by a fine glass capillary. For RNA-seq analysis, collagenase treatment was done at day 2 and COCs were collected at day 11 according to the previous method[12]. COCs were incubated in CTK (1 μM $CaCl_2$, 0.1 mg ml^{-1} collagenase type IV (MP Biomedicals), 20% KSR (Gibco) and 0.025% trypsin-EDTA (Gibco)) with 0.2 mM dibutyryl-cAMP (dbcAMP) (Sigma) and 0.1 mM 3-isobutyl-1-methylxanthine (IBMX) for 20 min at 37 °C and in Accutase (Nacalai Tesque) with dbcAMP and IBMX for 15 min at 37 °C. COCs were transferred to IVG manipulation medium supplemented with dbcAMP and IBMX and cumulus cells were strictly removed using a fine glass capillary. SC-positive oocytes were collected using a fluorescent microscope.

IVM culture

COCs were transferred to IVM medium (αMEM supplemented with 5% FCS, 25 μg ml^{-1} sodium pyruvate, 1× penicillin/streptomycin, 0.1 IU ml^{-1} FSH, 4 ng ml^{-1} EGF and 1.2 IU ml^{-1} hCG (ASKA)). At 16 h of culture, COCs were picked up for IVF or MII confirmation. For MII confirmation, swollen cumulus cells were stripped from the oocytes by treating with hyaluronidase (Sigma), and MII oocytes were determined by first polar body. For RNA-seq analysis, SC-positive oocytes were collected using a fluorescent microscope.

RNA sequencing analysis

A directional RNA-seq library was prepared as described previously[12]. In brief, PolyA+ RNAs were purified from oocytes (GV: 31–158; MII: 35–58) using a Dynabeads mRNA DIRECT Micro Kit (Invitrogen). Biologically duplicated samples in each stage were prepared. Purified RNAs were subjected to library preparation using a NEBNext Ultra II Directional RNA Library Prep Kit for Illumina (New England Biolabs). cDNAs were amplified by 13-cycle PCR. The libraries were sequenced on a NextSeq 500 DNA sequencer (75 bp single; Illumina). After trimming of adapter sequences and low-quality bases with Trimmomatic v.0.38[44], the processed reads were mapped to mouse genome mm10 using HISAT2 v.2.1.0[48]. Generated bam files were sorted and indexed using samtools v.1.9[46]. The number of reads mapped to each gene was counted with featureCounts v.2.0.0[49]. Low expressed genes (minimal counts per million: 0.5 in duplicates) were removed using edgeR v3.32.1[50] and scatter plots were generated using DESeq2 v1.30.1[51] in R.

IVF and embryo transfer

COCs after IVM were transferred to HTF medium (ARK Resource), and IVF was done as described previously[47]. Two-cell embryos were transferred into 0.5 days post coitum (dpc) pseudopregnant ICR females. Caesarean section was performed at 19.5 dpc and newborns were nursed by surrogate ICR mothers.

Germline transmission of iPS cells

Ten to twenty BV DsRed iPS cells were microinjected into BALB/c blastocysts. The blastocysts were transferred into the uterus of 2.5 dpc pseudopregnant ICR females. Male chimeras derived from XY iPS cells were mated with BALB/c females. Female chimeras derived from sex-converted XX iPS cells were mated with BALB/c males.

Genotyping

Genomic DNAs isolated from the tails or the placentas of the offspring from the sex-converted iPS cell-derived in vitro oocytes and chimeras were amplified by PCR for BV and DsRed transgenes, exogenous retroviral *Sox2* and *Pou5f1*, and wild-type *Prdm14* and then subjected to gel electrophoresis. The primers used in this genotyping are shown in Supplementary Table 1.

H-2K analysis

Male chimeras derived from XY iPS cells were mated with female chimeras derived from sex-converted XX iPS cells. Blood was obtained from the progenies and red blood cells were removed with ACK lysis buffer (150 mM NH_4Cl, 10 mM $KHCO_3$ and 0.1 mM EDTA). The remaining cells were stained with antibodies against H-$2K^b$ (FITC-conjugated, BioLegend, 1:250 dilution) and H-$2K^d$ (APC-conjugated, BioLegend, 1:250 dilution) according to the manufacturer's instruction. Lymphocytes in stained cells were selected and analysed using a FACSAria Fusion or FACSVerse flow cytometer with FACSuite v1.0.6 software (BD Biosciences). The antibodies used in this analysis are shown in Supplementary Table 2.

SNP genotyping

The Tyrp1 mRNA-UTR region of genomic DNAs isolated from the tails of the offspring between male chimera from XY iPS cells and female chimera from sex-converted XX iPS cells was amplified by PCR and then subjected to gel electrophoresis. PCR products excised from agarose gel were purified using a FastGene Gel/PCR Extraction Kit (NIPPON Genetics). Sanger sequencing was performed by GENEWIZ and SNPs (rs3022980 and rs3022981) were examined. The primers used in this genotyping are shown in Supplementary Table 1.

ES cell staining and generation of XX ES cells from XO ES cells with anti-CD38 antibodies

ES cells were stained with APC anti-CD38 antibody (BioLegend; 1:200 dilution) according to the manufacturer's instruction. To generate XX ES cells from XO ES cells, the APC-high population was sorted by a FACSAria Fusion cell sorter. The X-chromosome number of the sorted ES cells was examined by qPCR as described above. Detail of the anti-CD38 antibody is shown in Supplementary Table 2.

Immunofluorescence analysis

ES cells and day 3 PGCL cell aggregates were dissociated with incubation with trypsin-EDTA for 5 min at 37 °C, resuspended in 10% FBS/PBS and then spread on a slide glass for 2 min at 800 rpm with a Thermo Cytospin 4 (Thermo Fisher Scientific). Immunofluorescence staining was performed as described[52]. The slides were mounted in Fluoro-KEEPER Antifade Reagent for analysis using a LSM 700 laser scanning microscope (ZEISS). The primary and secondary antibodies used in this study are listed in Supplementary Table 2.

Reporting summary

Further information on research design is available in the Nature Portfolio Reporting Summary linked to this article.

Data availability

The DNA-seq data have been deposited at the Sequence Read Archive (SRA) database under accession number PRJNA766461 and the RNA-seq data have been deposited at the Gene Expression Omnibus (GEO) database under accession number GSE184771. Source data are provided with this paper.

Code availability

Custom code used in this article can be accessed at https://github.com/kentamurakami1986/oocytes-from-male-mice.

39. Ohta, H. et al. In vitro expansion of mouse primordial germ cell-like cells recapitulates an epigenetic blank slate. *EMBO J.* **36**, 1888–1907 (2017).
40. Ying, Q. L. et al. The ground state of embryonic stem cell self-renewal. *Nature* **453**, 519–523 (2008).
41. Hayashi, K. & Saitou, M. Generation of eggs from mouse embryonic stem cells and induced pluripotent stem cells. *Nat. Protoc.* **8**, 1513–1524 (2013).
42. D'Hulst, C., Parvanova, I., Tomoiaga, D., Sapar, M. L. & Feinstein, P. Fast quantitative real-time PCR-based screening for common chromosomal aneuploidies in mouse embryonic stem cells. *Stem Cell Rep.* **1**, 350–359 (2013).
43. Scheinin, I. et al. DNA copy number analysis of fresh and formalin-fixed specimens by shallow whole-genome sequencing with identification and exclusion of problematic regions in the genome assembly. *Genome Res.* **24**, 2022–2032 (2014).
44. Bolger, A. M., Lohse, M. & Usadel, B. Trimmomatic: a flexible trimmer for Illumina sequence data. *Bioinformatics* **30**, 2114–2120 (2014).
45. Li, H. & Durbin, R. Fast and accurate short read alignment with Burrows-Wheeler transform. *Bioinformatics* **25**, 1754–1760 (2009).
46. Danecek, P. et al. Twelve years of SAMtools and BCFtools. *Gigascience* **10**, giab008 (2021).
47. Hayashi, K., Hikabe, O., Obata, Y. & Hirao, Y. Reconstitution of mouse oogenesis in a dish from pluripotent stem cells. *Nat. Protoc.* **12**, 1733–1744 (2017).
48. Kim, D., Paggi, J. M., Park, C., Bennett, C. & Salzberg, S. L. Graph-based genome alignment and genotyping with HISAT2 and HISAT-genotype. *Nat. Biotechnol.* **37**, 907–915 (2019).
49. Liao, Y., Smyth, G. K. & Shi, W. featureCounts: an efficient general purpose program for assigning sequence reads to genomic features. *Bioinformatics* **30**, 923–930 (2014).
50. Robinson, M. D., McCarthy, D. J. & Smyth, G. K. edgeR: a Bioconductor package for differential expression analysis of digital gene expression data. *Bioinformatics* **26**, 139–140 (2010).
51. Love, M. I., Huber, W. & Anders, S. Moderated estimation of fold change and dispersion for RNA-seq data with DESeq2. *Genome Biol.* **15**, 550 (2014).
52. Sasaki, K. et al. Robust in vitro induction of human germ cell fate from pluripotent stem cells. *Cell Stem Cell* **17**, 178–194 (2015).

Acknowledgements We thank K. Kitajima and C. Meno for providing microscopes; N. Konishi for technical support; H. Toh for advice about DNA-seq; and Research Support Center, Research Center for Human Disease Modeling, Kyushu University Graduate School of Medical Sciences for technical assistance. This study was supported in part by Grant-in-Aid for Scientific Research on Innovative Areas from JSPS (grants 18H05544 and 18H05545 to K.H. and 18H05549 to T.S.K.); by a Grant-in-Aid for Specially Promoted Research from JSPS (grants 17H06098 and 22H04920 to M.S.); by the Takeda Science Foundation (K.H.); by the Luca Bella Foundation (K.H.); and by a Grant-in-Aid from The Open Philanthropy Project (K.H.).

Author contributions K.H. conceived the project. K.M., N. Hamazaki and K.H. performed the investigation. N. Hamazaki, T.S.K. and I.O. contributed the methodology. K.M. performed the DNA-seq and RNA-seq analyses. N. Hamada, G.N., H.O., Y.N., Y.I., Y.S., Y.K., F.A., K.A. and M.S. provided the resources. K.K. and K.H. supervised the project. K.M. and K.H. wrote the manuscript, incorporating feedback from all the authors.

Competing interests K.H. is an inventor on patent applications relating to in vitro oocyte production in mice filed by Kyushu University.

Additional information

Supplementary information The online version contains supplementary material available at https://doi.org/10.1038/s41586-023-05834-x.

Correspondence and requests for materials should be addressed to Katsuhiko Hayashi.

Peer review information *Nature* thanks Diana Laird and the other, anonymous, reviewer(s) for their contribution to the peer review of this work. Peer review reports are available.

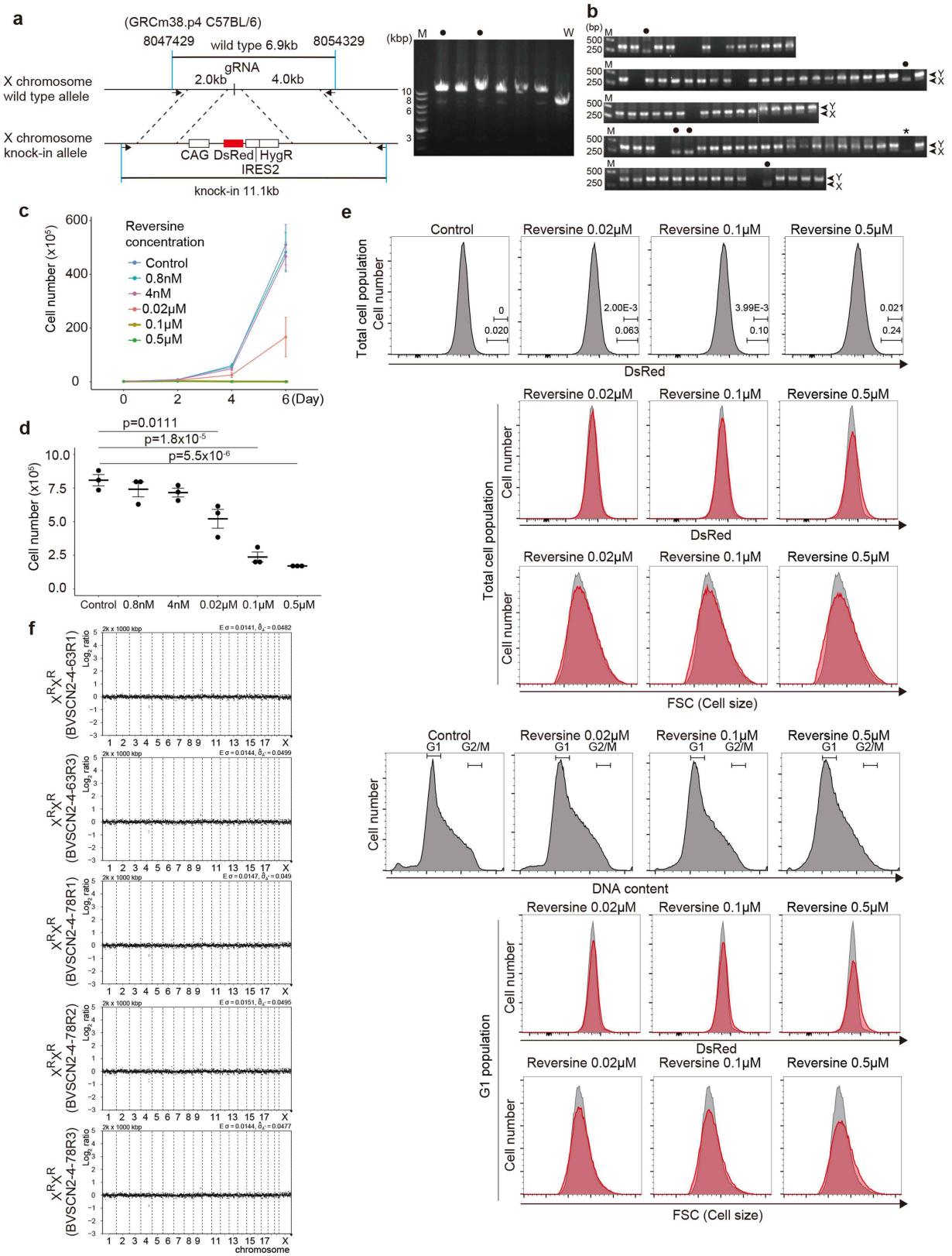

Extended Data Fig. 1 | See next page for caption.

Extended Data Fig. 1 | Generation of XX ES cells from XO ES cells with reversine. (**a**) Knock-in of DsRed into the X chromosome. The schematic diagram shows the gRNA position, primers for genotyping (arrows), and expected sizes of the amplicons. The right image shows the result of PCR using the primers. The black dots indicate the ES cell lines used in this study. M, size marker. W, wild type. (**b**) Removal of the Y chromosome. Shown are the results of PCR analysis of sex chromosomes. Each sex chromosome is indicated at the left side of the image. Black dots indicate XO ES cell clones. The lane with an asterisk was excluded from the count because the band was faint. (**c**) Effect of reversine on the proliferation of ES cells at each passage. The results of three independent experiments are shown as mean±s.e.m. (**d**) The effect of reversine treatment on the proliferation of ES cells at day 2. The results of three independent experiments are shown as mean±s.e.m. *P* value was determined by One-way ANOVA with Bonferroni adjustment. (**e**) Effect of reversine on DsRed intensity of X^RO ES cells in the total cell population and G1 population. The top row shows the DsRed intensity of the total cell population cultured without (Control) or with reversine at each concentration. The numbers show the percentage of the cell population at each reversine concentration. The second row shows the overlay of the DsRed intensity of the total cell population cultured without (grey) and with reversine (red) at each concentration. The third row shows the overlay of the cell size measured by forward scatter (FSC) of the total cell population cultured without (grey) and with reversine (red) at each concentration. The fourth row shows the DNA content in the total cell population cultured without (Control) or with reversine at each concentration. The G1 population in each plot was analyzed in the fifth and bottom rows. The fifth row shows the overlay of the DsRed intensity of the G1 population cultured without (grey) and with reversine (red) at each concentration. The bottom row shows the overlay of the cell size measured by forward scatter (FSC) of the G1 population cultured without (grey) and with reversine (red) at each concentration. Note that DsRed-highly positive cells increased in proportion to the concentration of reversine in both the total cell and G1 populations, whereas the cell size became diverse in both the small and large fractions. (**f**) DNA-seq analysis of sex-converted ES cell clones. Shown are the results of sex-converted ES cell clones apart from the ES cell clone shown in Fig. 1e. Two copies are plotted at 0 in $\log_2$ ratio. The numbers below the plot are the chromosome numbers.

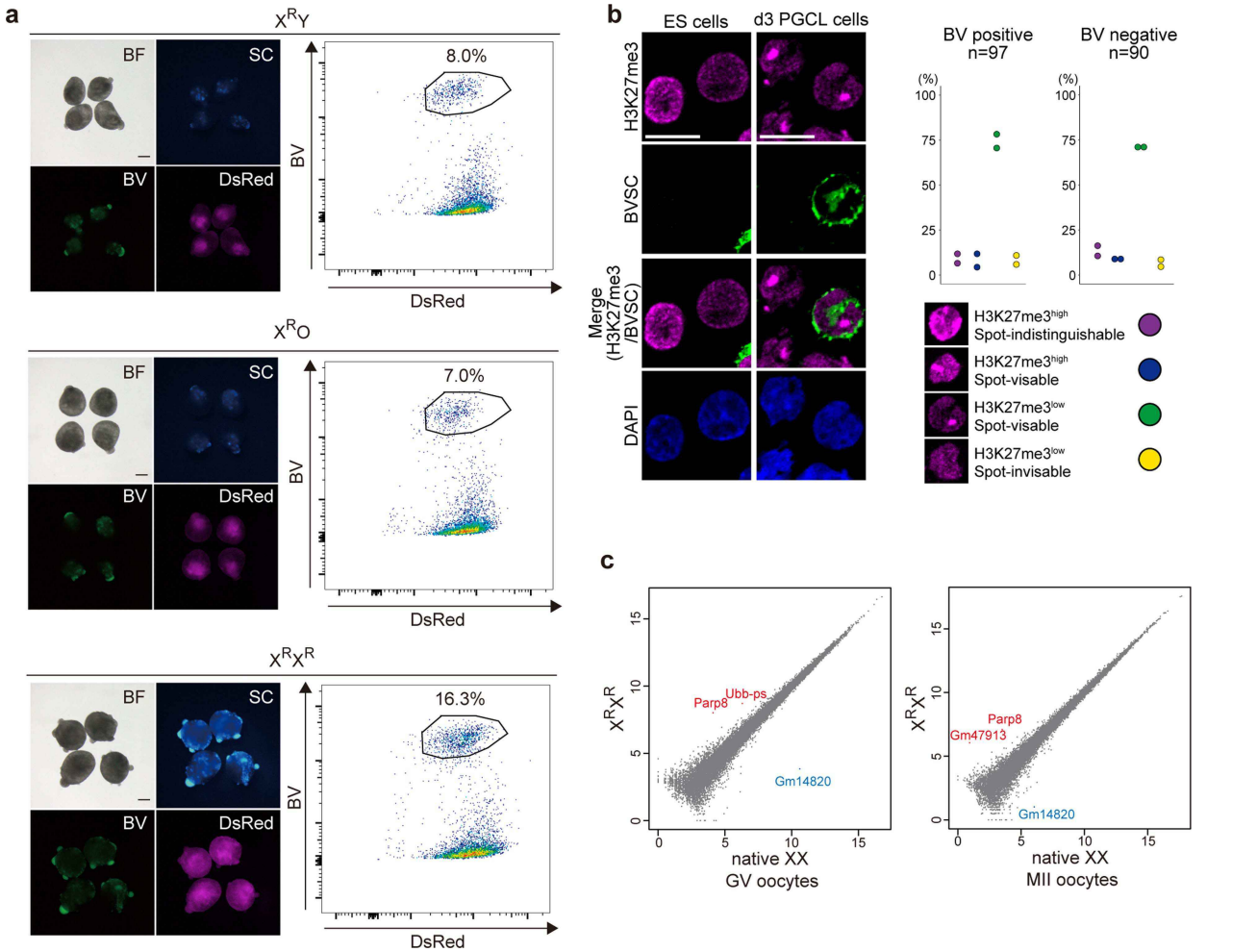

Extended Data Fig. 2 | PGCL cell induction and transcriptome analysis of oocytes from the sex-converted XX ES cells. (**a**) PGCL cell induction from X^RY, X^RO and X^RX^R ES cells. The numbers in the FACS analysis images are the percentages of PGCL cells. Scale bars, 200 µm. (**b**) H3K27me3 states indicative of X chromosome states during PGCL cell induction. Images show immunofluorescence analysis of ES cells and PGCL cells at day 3 of induction (d3 PGCL cells). Note that single H3K27me3 bright spots corresponding to Xi, were observed in cells at day 3 of PGCL cell induction. Scale bars, 10 µm. The right graph shows the percentage of cells with the indicated H3K27me3 state in BV positive and negative cells at day 3 of PGCL cell induction. These results are based on biologically duplicated samples. (**c**) Gene expression analysis of GV (left) and MII (right) oocytes differentiated from native XX ES cells (BVSCH18) and X^RX^R ES cells (BVSCN2-4-63R2). Genes expressed more than twofold higher (red) or twofold lower (blue) in X^RX^R oocytes are shown. The FDR cutoff is 0.01. Biological duplicate samples.

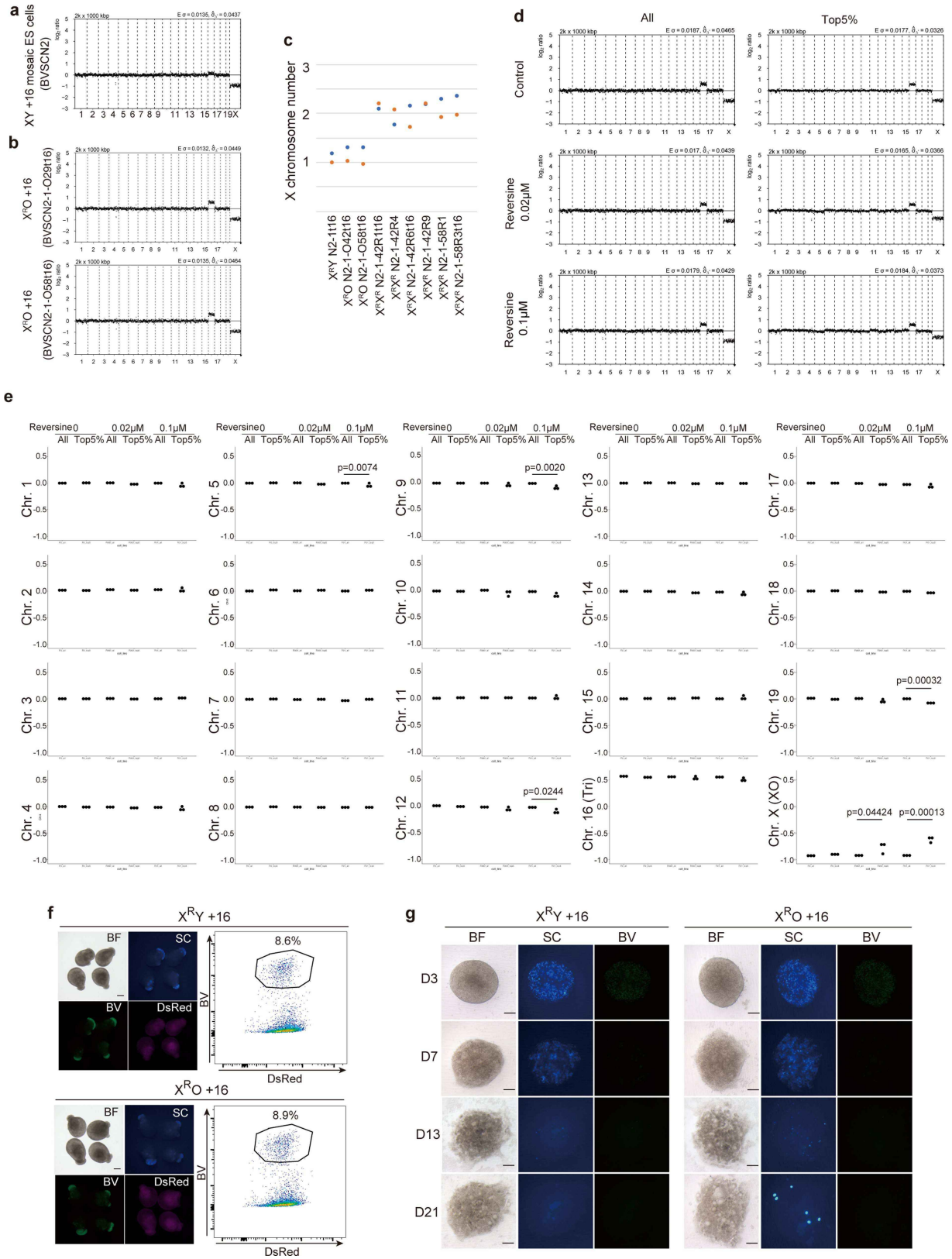

Extended Data Fig. 3 | See next page for caption.

Extended Data Fig. 3 | Reversine effect on trisomy 16 ES cells and oocyte production from trisomy 16 XY and XO ES cells. (**a**) DNA-seq analysis of a mosaic trisomy 16 clone. (**b**) DNA-seq analysis of trisomy 16 X^RO ES cells. Another trisomy 16 X^RO cell line is shown in Fig. 2b. (**c**) Q-PCR analysis to determine the X chromosome number. Blue and orange dots show the X chromosome content determined using chromosome 7 and chromosome 11, respectively, as references. Details are described in Fig. 1c. The genotypes of sex chromosomes and individual clone IDs are shown below the graph. (**d**) DNA-seq analysis of FACS sorted trisomy 16 X^RO ES cells without (control) or with reversine treatment. The left column shows the whole population, and the right column shows the top 5% fraction of the DsRed-high population. (**e**) Log_2 ratio of autosomes and the X chromosome under each condition in the DNA-seq analysis. Note that the ratio of X^RX^R ES cells was significantly increased in the top 5% fraction compared to the total cell fraction with 0.02 μM reversine, while autosomes were relatively unaffected. There was no significant difference ($P > 0.11$) in the ratio of X^RX^R ES cells in the top 5% fraction without and with 0.02 μM reversine, consistent with the results shown in Fig. 1b. *P* value was determined by One-way ANOVA with Bonferroni adjustment. The values were compiled from biologically triplicated experiments. (**f**) PGCL cell induction from trisomy 16 X^RY ES cells and trisomy 16 X^RO ES cells. Shown are representative images and FACS analyses of the induction of PGCL cells from the ES cells indicated. The numbers in the FACS analysis are the percentages of PGCL cells. Scale bars, 200 μm. (**g**) IVDi culture using PGCL cells from trisomy 16 X^RY ES cells and trisomy 16 X^RO ES cells. Representative images of the rOvaries at the days indicated are shown. Scale bars, 200 μm. Similar results were obtained in biologically duplicated experiments.

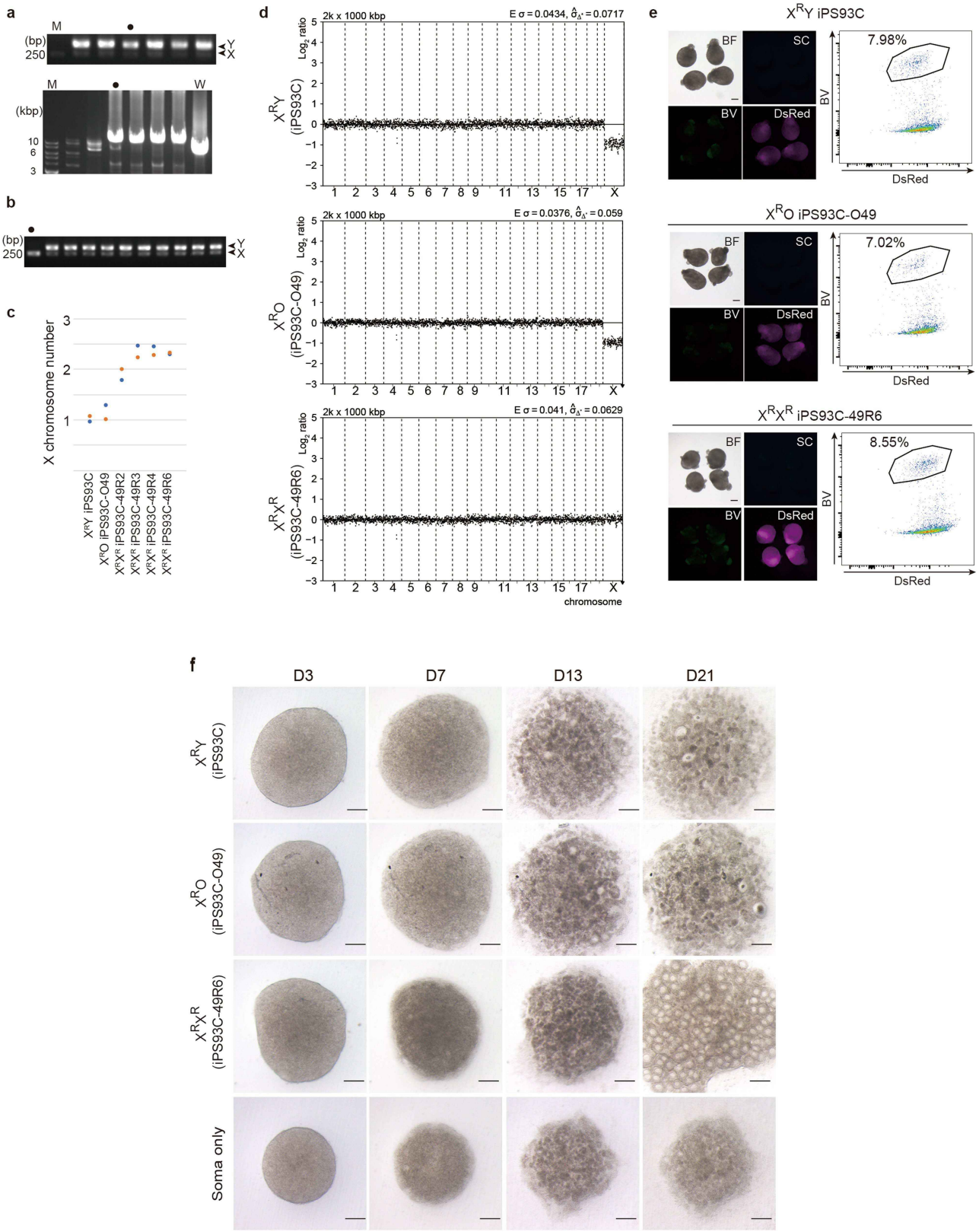

Extended Data Fig. 4 | See next page for caption.

Extended Data Fig. 4 | Generation of XX iPS cells from XY iPS cells followed by oocyte production. (**a**) Genotype of XY iPS cells used in this study. Shown are the results of PCR analysis of sex chromosomes (top) and knock-in of DsRed into the X chromosome (bottom). Details for the knock-in are shown in Extended Data Fig. 1a. All six iPS cell lines tested had X and Y chromosomes (top). The black dot in each image indicates the iPS cell clone used in this study. The knock-in alleles were detected in four of the six iPS cell lines. The same results were obtained in PCR experiment repeated twice. (**b**) Removal of the Y chromosome. Shown are the results of PCR analysis of sex chromosomes after 9 passages. The black dot indicates X^RO iPS cells used in this study. The same results were obtained in PCR experiment repeated twice. (**c**) Q-PCR analysis to determine the X chromosome number. Blue and orange dots show the X chromosome content determined using chromosome 7 and chromosome 11, respectively, as references. Details are described in Fig. 1c. The genotypes of sex chromosomes and individual clone IDs are shown below the graph. (**d**) DNA-seq analysis of sex-converted iPS cell clones. Two copies are plotted at 0 in $\log_2$ ratio. The numbers below the plot are the chromosome numbers. The genotypes and the IDs of the individual clones are displayed on the left side of the plot. (**e**) PGCL cell induction from X^RY, X^RO and X^RX^R iPS cells. Shown are representative images and FACS analyses of the induction of PGCL cells from the iPS cells indicated. The numbers in the FACS analysis are the percentages of PGCL cells. Scale bars, 200 μm. Similar results were obtained in biologically duplicated experiments. (**f**) IVDi culture using PGCL cells from X^RY, X^RO and X^RX^R iPS cells. Shown are representative images of the rOvaries at the days indicated. As a negative control, a representative rOvary containing only embryonic gonadal somatic cells is shown. The images at day 21 of culture are the same as in Fig. 3b. Scale bars, 200 μm. Similar results were obtained in biologically duplicated experiments.

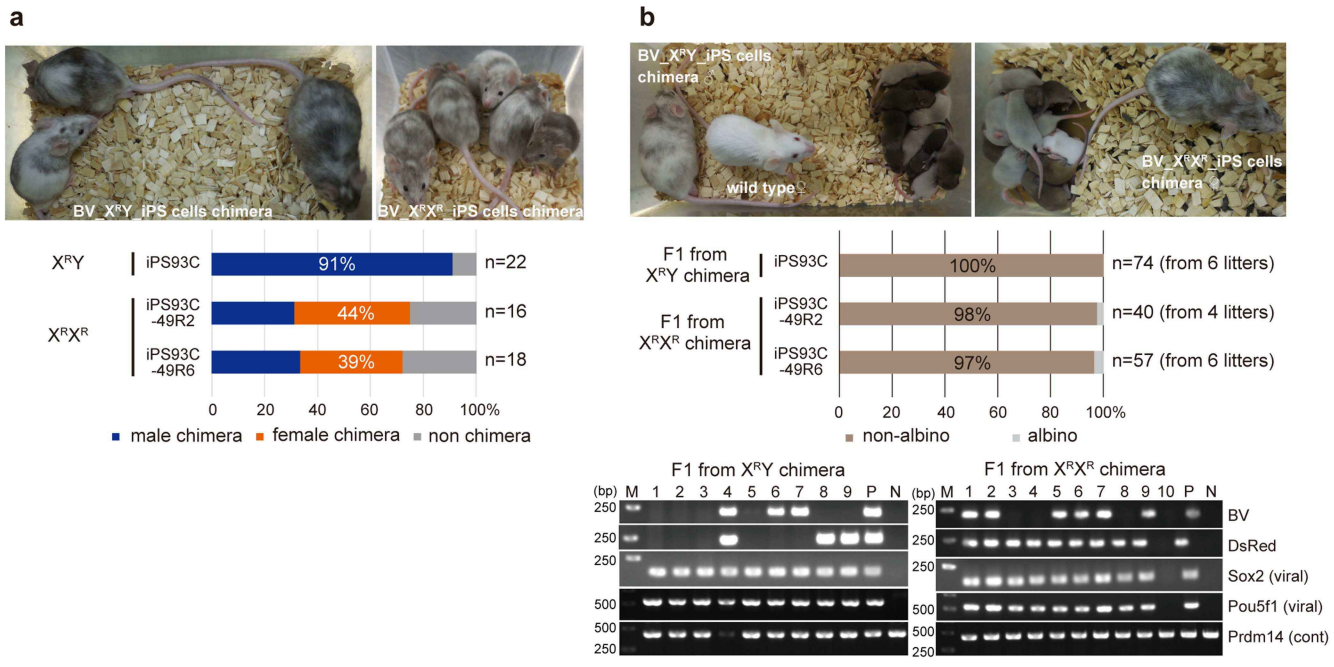

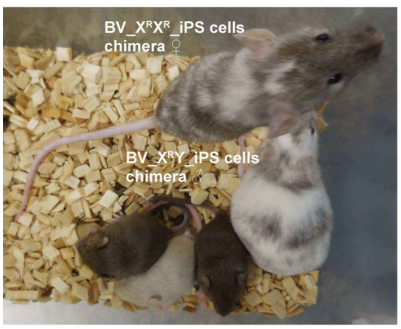

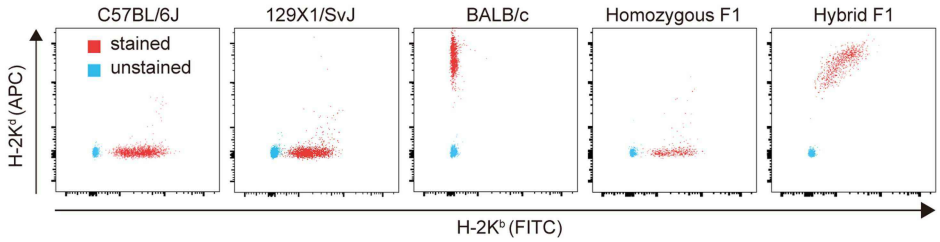

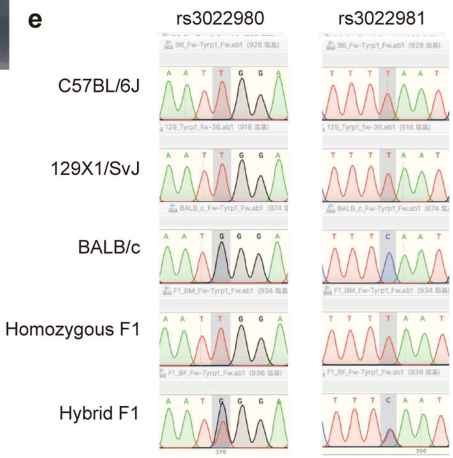

f

Chimeric cell line (XRY)	(XRXR)	Total F1	Homozygous F1 (%)
iPS93C x	iPS93C-49R2	14	2 (14)
iPS93C x	iPS93C-49R6	3	2 (67)

Extended Data Fig. 5 | See next page for caption.

Extended Data Fig. 5 | Derivation of offspring from a single iPS cell line. (**a**) Chimeric mice harbouring X^RY or sex-converted X^RX^R iPS cells. The graph below the images shows the ratio of iPS cell chimeric mice. The number in the top graph is the percentage of male chimeras harbouring X^RY iPS cells and the numbers in the middle and bottom graphs are the percentages of female chimeras harbouring X^RX^R iPS cells. (**b**) Offspring from chimeric mice harbouring X^RY or sex-converted X^RX^R iPS cells. The top images show offspring from male chimeric mice harbouring X^RY iPS cells (left) and offspring female chimeric mice harbouring X^RX^R iPS cells (right). The middle graph shows the coat colour of offspring from a mating between chimeric mice and wild-type albino mice. The number in the graph is the percentage of non-albino mice from a mating between chimeric mice and wild type albino mice. The bottom gel image show genotyping of the offspring from iPS cell chimeric mice harbouring X^RY iPS cells (left) or sex-converted X^RX^R iPS cells (right). PCR products from *BV* and *DsRed* transgenes, exogenous retroviral *Sox2* and *Pou5f1*, and the *Prdm14* locus as a positive control are shown. The coat colour of number 10 was albino. P, positive control. N, negative control. Details of the positive control and negative control are described in Fig. 3d. (**c**) Pups from a mating between an X^RY iPS cell-chimeric male and X^RX^R iPS cell-chimeric female mouse. (**d**) FACS analysis of H-2K haplotypes of offspring obtained from crosses between the chimeric mice. Shown are the FACS plot of H-2K haplotypes in lymphocytes of C57BL/6J ($H\text{-}2K^b$), 129X1/SvJ ($H\text{-}2K^b$), Balb/c ($H\text{-}2K^d$), and F1 mice from a mating between chimeric mice. Note that one of the F1 mice had only $H\text{-}2K^b$, whereas the other had a hybrid haplotype. (**e**) SNP analysis of offspring. Shown are SNPs at rs3022980 and rs3022981 in C57BL/6J, 129X1/SvJ, BALB/c and F1 mice from a mating between chimeric mice. (**f**) Ratio of homozygous F1 from a mating between an X^RY iPS cell-chimeric mouse and X^RX^R iPS cell-chimeric mouse. (**g**) An adult mouse from (**c**) at 10 months after birth.

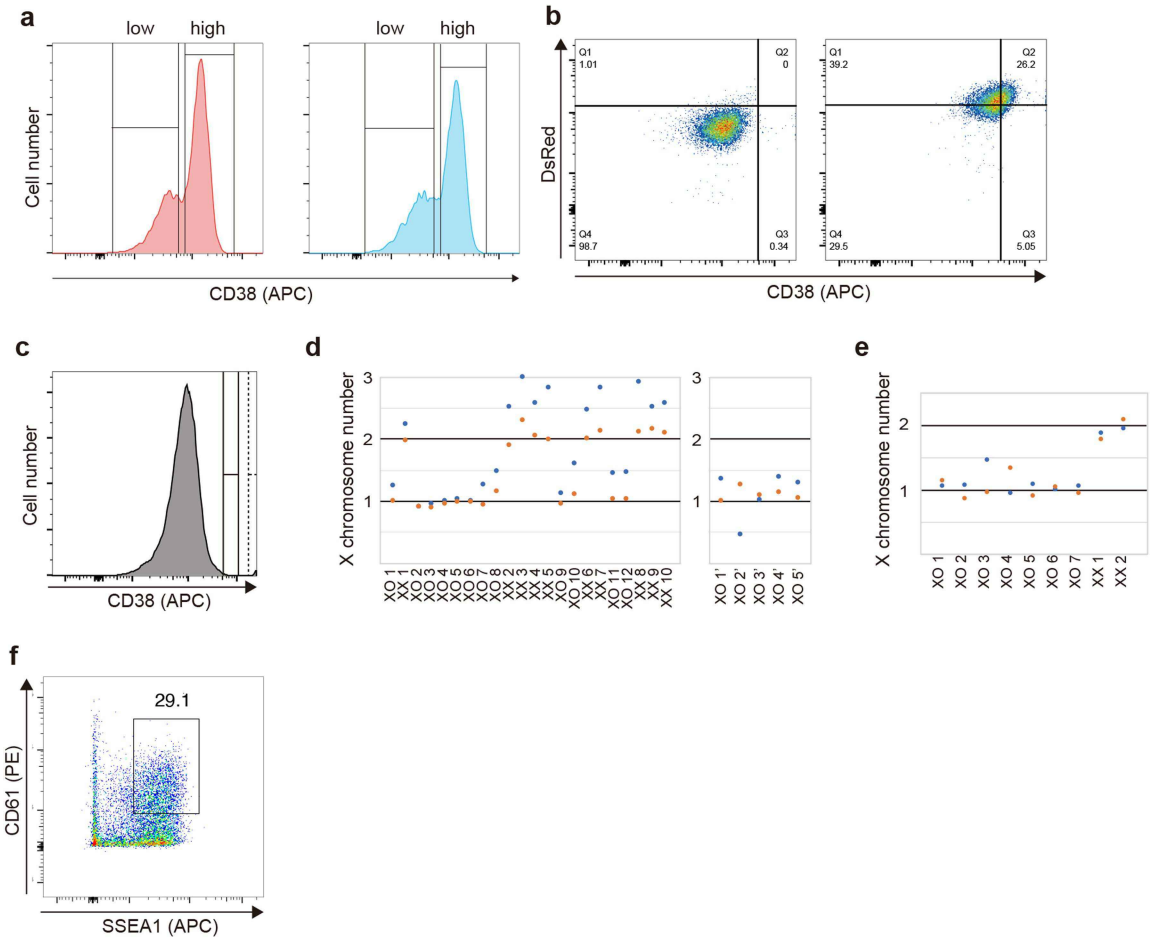

Extended Data Fig. 6 | Generation of XX ES cells from XO ES cells using anti-CD38 antibodies. (**a**) FACS analysis of CD38 expression in C57BL/6J (originally XX) ES cells. Note that there are two types of CD38 expression: low and high. (**b**) FACS analysis of DsRed and CD38 in X^RO and X^RX^R ES cells. Note that the CD38 intensity was increased in X^RX^R ES cells in proportion to the intensity of DsRed. (**c**) The gates used to select XX ES cells from XO ES cells using anti-CD38 antibodies. The gate at left (solid line) was used for the CD38-high cell population and the gate at right (dashed line) was used for the CD38-extremely high cell population. (**d**) Q-PCR analysis to determine the X chromosome number. The left graph shows the results using BVSC XO ES cells with high CD38 (the solid gate in (**c**)) and the right graph shows the results using BVSC XO ES cells with extremely high CD38 (the dashed gate in (**c**)). (**e**) The graph shows the results using non-reporter XO ES cells with high CD38. The genotypes of sex chromosomes and individual clone IDs are shown below the graph. Blue and orange dots show the X chromosome content determined using chromosome 7 and chromosome 11, respectively, as references. Details are described in Fig. 1c. (**f**) FACS analysis of PGCL cells derived from non-reporter and X-duplicated ESCs. PGCL cells were identified by antibodies against SSEA1 and CD61[26]. Similar results were obtained in biologically duplicated experiments.

Extended Data Table 1 | Frequency of Y-chromosome loss in XY ES cells and iPS cells

Cell line	Total subclones screened	Y negative subclones (%)
BVSCN2-4 (Extended Data Fig. 1b)	87	5 (5.7)
BVSCN2-1t16 (XY ESCs with 16 trisomy)	90	3 (3.3)
iPS93C (Extended Data Fig. 4b)	91	1 (1.1)

The total numbers of subclones screened and the number of subclones lacking the Y chromosome are shown. The loss of the Y chromosome was confirmed by PCR.

Extended Data Table 2 | Percentage of MII oocytes after IVM

Cell line		Collected COCs	MII oocytes (% of collected COCs)
BVSCN2-4-63R2	Experiment 1	73	10
(Figure 1)	Experiment 2	125	55
	Experiment 3	151	43
	Total	349	108 (30.9)
BVSCN2-1-42R4	Experiment 1	92	10 (10.9)
(Figure 2)			
BVSCN2-1-42R9	Experiment 1	244	42 (17.2)
(Figure 2)			
iPS93C-49R6	Experiment 1	110	40
(Figure 3)	Experiment 2	105	48
	Experiment 3	74	33
	Total	289	121 (41.9)

The numbers of collected COCs and MII oocytes per each experiment are shown. The numbers in parentheses indicate the percentage of MII oocytes in the collected COCs.

Extended Data Table 3 | Percentage of 2-cell embryos after IVF using iPS93C-49R6

	Collected COCs	2-cell embryos (% of COCs)
Experiment 1	466	197
Experiment 2	225	71
Experiment 3	337	117
Total	1028	385 (37.5)

The numbers of collected COCs and 2-cell embryos per each experiment are shown. The number in parentheses indicates the percentage of 2-cell embryos in the collected COCs.

Extended Data Table 4 | Birth rate of the 2-cell embryos transferred using iPS93C-49R6

	2-cell embryos transferred	Pups (% of 2-cell embryos transferred)
Experiment 1	87	1 (1.1)
Experiment 2	32	0 (0.0)
Experiment 3	79	0 (0.0)
Experiment 4	103	0 (0.0)
Experiment 5	109	1 (0.9)
Experiment 6	93	0 (0.0)
Experiment 7	127	2, 3 (3.9)
Total	630	7 (1.1)

The numbers of 2-cell embryos transferred and pups per each experiment are shown. The numbers in parentheses indicate the percentage of pups in the 2-cell embryos transferred.

nature portfolio

Corresponding author(s): Katsuhiko Hayashi

Last updated by author(s): Feb 2, 2023

Reporting Summary

Nature Portfolio wishes to improve the reproducibility of the work that we publish. This form provides structure for consistency and transparency in reporting. For further information on Nature Portfolio policies, see our Editorial Policies and the Editorial Policy Checklist.

Statistics

For all statistical analyses, confirm that the following items are present in the figure legend, table legend, main text, or Methods section.

n/a	Confirmed	
☐	☒	The exact sample size (*n*) for each experimental group/condition, given as a discrete number and unit of measurement
☐	☒	A statement on whether measurements were taken from distinct samples or whether the same sample was measured repeatedly
☐	☒	The statistical test(s) used AND whether they are one- or two-sided *Only common tests should be described solely by name; describe more complex techniques in the Methods section.*
☒	☐	A description of all covariates tested
☒	☐	A description of any assumptions or corrections, such as tests of normality and adjustment for multiple comparisons
☐	☒	A full description of the statistical parameters including central tendency (e.g. means) or other basic estimates (e.g. regression coefficient) AND variation (e.g. standard deviation) or associated estimates of uncertainty (e.g. confidence intervals)
☐	☒	For null hypothesis testing, the test statistic (e.g. *F*, *t*, *r*) with confidence intervals, effect sizes, degrees of freedom and *P* value noted *Give P values as exact values whenever suitable.*
☒	☐	For Bayesian analysis, information on the choice of priors and Markov chain Monte Carlo settings
☒	☐	For hierarchical and complex designs, identification of the appropriate level for tests and full reporting of outcomes
☒	☐	Estimates of effect sizes (e.g. Cohen's *d*, Pearson's *r*), indicating how they were calculated

Our web collection on statistics for biologists contains articles on many of the points above.

Software and code

Policy information about availability of computer code

Data collection	No software was used except for Illumina basecalling and demultiplexing software.
Data analysis	Freely available softwares were used to analyze DNA or RNA sequencing data, as described in Methods: Trimmomatic_0.38, bwa_0.7.17, samtools_1.9, Picard_2.18.12, QDNAseq_1.26.0, HISAT2_2.1.0, featureCounts_2.0.0, edgeR_3.32.1 and DESeq2_1.30.1, R_4.0.4. FACS data were analyzed by FACSDiva_6.1.3, FACSuite_1.0.6 and Flowjo_10.5.3. Custom code used in this article can be accessed on https://github.com/kentamurakami1986/oocytes-from-male-mice.

For manuscripts utilizing custom algorithms or software that are central to the research but not yet described in published literature, software must be made available to editors and reviewers. We strongly encourage code deposition in a community repository (e.g. GitHub). See the Nature Portfolio guidelines for submitting code & software for further information.

Data

Policy information about availability of data

All manuscripts must include a data availability statement. This statement should provide the following information, where applicable:

- Accession codes, unique identifiers, or web links for publicly available datasets
- A description of any restrictions on data availability
- For clinical datasets or third party data, please ensure that the statement adheres to our policy

All data shown in this study can be downloaded in raw and processed forms from the NCBI Sequence Read Archive (PRJNA766461) and the NCBI Gene Expression Omnibus (GSE184771). The raw data are associated with Figures 1e, 2b and Extended Data Figures 1f, 2b, 3a, 3b, 3d, 4d. There is no restriction on data availability.

Human research participants

Policy information about studies involving human research participants and Sex and Gender in Research.

Reporting on sex and gender	There is no human research participant in this study
Population characteristics	There is no human research participant in this study
Recruitment	There is no human research participant in this study
Ethics oversight	There is no human research participant in this study

Note that full information on the approval of the study protocol must also be provided in the manuscript.

Field-specific reporting

Please select the one below that is the best fit for your research. If you are not sure, read the appropriate sections before making your selection.

☒ Life sciences ☐ Behavioural & social sciences ☐ Ecological, evolutionary & environmental sciences

For a reference copy of the document with all sections, see nature.com/documents/nr-reporting-summary-flat.pdf

Life sciences study design

All studies must disclose on these points even when the disclosure is negative.

Sample size	No statistical method was used to predetermined sample size. Sample sizes were determined to obtain reproducibility and reliable destribution among biologically independent samples, based on extensive laboratory experience and literatures in this field (Li et al. Nature, 564: 136-140, 2018; Ohta et al. EMBO J 36: 1888-1907, 2017).
Data exclusions	No data were excluded from the study.
Replication	We made biological duplicates or more for all samples to be tested in the experiments in this study. All attempts at replication were successful.
Randomization	The experiments were not randomized as we tested all available samples.
Blinding	Sequencing and sample collection were performed by more than two different reasearchers. Sample names and group allocations were blinded during data collection. The investigators were not blinded during data analyisis, due to feasibility of data analysis.

Reporting for specific materials, systems and methods

We require information from authors about some types of materials, experimental systems and methods used in many studies. Here, indicate whether each material, system or method listed is relevant to your study. If you are not sure if a list item applies to your research, read the appropriate section before selecting a response.

Materials & experimental systems

n/a	Involved in the study
☐	☒ Antibodies
☐	☒ Eukaryotic cell lines
☒	☐ Palaeontology and archaeology
☐	☒ Animals and other organisms
☒	☐ Clinical data
☒	☐ Dual use research of concern

Methods

n/a	Involved in the study
☒	☐ ChIP-seq
☐	☒ Flow cytometry
☒	☐ MRI-based neuroimaging

Antibodies

Antibodies used

All antibodies are commercially available.
FACS
FITC anti-mouse H-2Kb, Mouse, BioLegend, 116505, 1:250 dilution
APC anti-mouse H-2Kd, Mouse, BioLegend, 116619, 1:250 dilution
APC anti-mouse CD38, Rat, BioLegend, 102711, 1:200 dilution
APC anti-mouse/human CD15, Mouse, BioLegend, 125617, 1:20
PE anti-mouse /rat CD61, Hamster, BioLegend, 104307, 1:200

MACS
Anti-SSEA-1 (CD15) MicroBeads, human and mouse, Mouse, Miltenyi Biotec, 130-094-530, 1:10 dilution
Anti-CD31 MicroBeads, Rat, Miltenyi Biotec, 130-097-418, 1:10 dilution

Immunofluorescence analysis
Anti-Anti-H3K27me3 (C36B11), Rabbit, Cell Signaling Technology, 9733, 1:500
Anti-GFP, Chicken, Abcam, ab13970, 1:500
Goat anti-Chicken IgG Alexa Fluor 488, Goat, Thermo Fisher Scientific, A11039, 1:500
Donkey anti-Rabbit IgG Alexa Fluor 568, Donkey, Thermo Fisher Scientific, A10042, 1:500

Validation

Validation statements of all antibodies are available in the manufacturers websites (www.biolegend.com; www.miltenyibiotec.com; www.cellsignal.jp; www.abcam.co.jp; www.thermofisher.com).

Eukaryotic cell lines

Policy information about cell lines and Sex and Gender in Research

Cell line source(s)

BVSCN2, BVSCH18 and BCF1 ESCs were obtained from Dr. Mitinori Saitou (Kyoto University). C57BL/6J and F1(129X1/SvJxC57BL/6/J) ESCs and iPSCs were made by ourselves.

Authentication

Transgenes (BV and SC) and sex chromosomes of the cell lines were tested by genomic PCR at their establishment from mice embryos. Proper knock-in of DsRed was confirmed by genomic PCR.

Mycoplasma contamination

The cell lines were not tested for Mycoplasma contamination.

Commonly misidentified lines
(See ICLAC register)

No commonly misidentified cell lines were used.

Animals and other research organisms

Policy information about studies involving animals; ARRIVE guidelines recommended for reporting animal research, and Sex and Gender in Research

Laboratory animals

This study used ICR mice for collection of gonadal somatic cells and sperm, C57BL/6 and 129X1/SvJ mice for collection of blood, F1(129X1/SvJ x C57BL/6) mice for generation of IPSCs and BALB/c mice for collection of blastocysts. Mice used for collection of sperm were males older than 12 weeks of age. Mice used for collection of blood were males older than 4 weeks of age. Mice used for collection of gonadal somatic cells or blastocysts were females older than 8 weeks of age. All mice were maintained in constant temperature (22-25°C) and humidity (50-70%) under a 12h light-12h dark cycle with light onset at 8am.

Wild animals

The study did not involve wild animals.

Reporting on sex

Sex of animals used in this study is described.

Field-collected samples

The study did not involve samples collected from the field.

Ethics oversight

All animal experiments were performed under the ethical guidelines of Kyushu University for animal use (#A20-026-1 and #20-009-1).

Note that full information on the approval of the study protocol must also be provided in the manuscript.

Flow Cytometry

Plots

Confirm that:

☒ The axis labels state the marker and fluorochrome used (e.g. CD4-FITC).

☒ The axis scales are clearly visible. Include numbers along axes only for bottom left plot of group (a 'group' is an analysis of identical markers).

☒ All plots are contour plots with outliers or pseudocolor plots.

☒ A numerical value for number of cells or percentage (with statistics) is provided.

Methodology

Sample preparation	The cells were dissociated by trypsin digestion and gentle pipetting and filtered by using a 70 µm-pored nylon mesh to remove cell clumps.
Instrument	FACSAria SORP, FACSAria Fusion, or FACSVerse
Software	FACSDiva (version 6.1.3), FACSuite (version 1.0.6) and FlowJo (version 10.5.3) were used for data collection and analysis.
Cell population abundance	The purity of sorted cells were confirmed by their reporter fluorescence activity, e.g. Stella-ECFP, Blimp1-mVenus, and DsRed under inverted microscopy.
Gating strategy	FSC-A and SSC-A scatter plot were used to separate cell events from debris and/or dead cells. FSC-H, FSC-W, SSC-H, and SSCW were used to separate singlets and doublets. These gating strategies are provided in Supplementary Figures.

☒ Tick this box to confirm that a figure exemplifying the gating strategy is provided in the Supplementary Information.